GUIDEBOOK

The Badenian evaporative stage of the Polish Carpathian Foredeep: sedimentary facies and depositional environment of the selenitic Nida Gypsum succession

Guide to field trip A2 • 21–22 June 2015

Maciej Bąbel, Danuta Olszewska-Nejbert, Krzysztof Nejbert, Damian Ługowski

31st IAS
Meeting of Sedimentology
Kraków, Poland • June 2015

ORLEN Upstream

www.orlenupstream.pl

DRILLING

RESERVOIR ENGINEERING

E&P PROJECT ANALYSIS

PRODUCTION PROCESSES

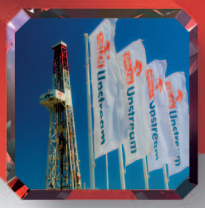

GEOLOGY

GEOPHYSICS

ENVIRONMENTAL PROTECTION HSE

ORLEN GROUP. FUELLING THE FUTURE.

ORLEN Upstream Sp. z o.o.
ul. Prosta 70 | 00-838 Warszawa
Tel.: +48 22 778 02 00 | Fax: +48 22 395 49 69

The Badenian evaporative stage of the Polish Carpathian Foredeep: sedimentary facies and depositional environment of the selenitic Nida Gypsum succession

Maciej Bąbel[1], Danuta Olszewska-Nejbert[1], Krzysztof Nejbert[1], Damian Ługowski[1]

[1]Faculty of Geology, University of Warsaw
(m.babel@uw.edu.pl, don@uw.edu.pl, knejbert@uw.edu.pl, lugowski.damian@gmail.com)

Route (Fig. 1): From Kraków we drive NE by road 776 to Skalbmierz, then by road 768 to Działoszyce, where we turn onto road 64T to Chroberz. Then by local roads we arrive to the hill near abandoned quarry at **Gacki (A2.1)**. From Gacki we follow east by local roads (ca. 2 km) to the **Leszcze quarry (A2.2)**. From Leszcze south by local roads (ca. 4 km) to **Zagość-Winiary road cut** in the escarpment of the Nida river valley **(A2.3)**. Then by local roads through Skorocice and Siesławice to Busko-Zdrój (ca. 12 km), to hotel "Gromada", Waryńskiego 10. From Busko-Zdrój by local roads to SW, to abandoned quarries at **Siesławice (A2.4)**. From Siesławice to SW by road 973 to the round-about crossing with 776, where we turn right. After ca. 9 km we turn east onto local roads to abandoned gypsum stone pits at Góry Wschodnie nature reserve at **Chotel Czerwony-Zagórze (A2.5)**. After returning to road 776 we continue south to the town of Wiślica (car parks) and walk to **Wiślica-Grodzisko (A2.6)** at the SE outskirts of the town. From Wiślica we drive to NW by local roads to Krzyżanowice Dolne (lunch at OSW Zacisze). From Krzyżanowice Dolne we drive N by local roads through Kowala to Pasturka, then NW by road 767 to Pińczów and by local roads through Włochy to the **Borków quarry (A2.7)**. From Borków eastward by local roads through Pińczów to road 7 (E77) and we follow it to Kraków.

Introduction to the trip

The Nida Gypsum deposits – the record of the Badenian salinity crisis in the northern margin of the Carpathian Foredeep Basin

Maciej Bąbel, Danuta Olszewska-Nejbert

Introduction

The Badenian salinity crisis, known also as the Wielician crisis, was a crucial event in the Miocene history of the Central Paratethys. The Middle Miocene (Badenian) seas occupying the area of the emerging Carpathian orogen lost their open connection with the Mediterranean Sea and were transformed into evaporite basins (Fig. 2A; Peryt, 2006). The widespread evaporite deposition has taken place at that time in the Carpathian Foredeep Basin developing in front of the advancing Carpathian thrust belt (Oszczypko *et al.*, 2006). In this basin gypsum deposits were formed mainly on the broad platformal marginal zone (Fig. 2B).

Bąbel, M., Olszewska-Nejbert, D., Nejbert, K. & Ługowski, D., 2015. The Badenian evaporative stage of the Polish Carpathian Foredeep: sedimentary facies and depositional environment of the selenitic Nida Gypsum succession. In: Haczewski, G. (ed.), *Guidebook for field trips accompanying IAS 31st Meeting of Sedimentology held in Kraków on 22nd–25th of June 2015*. Polish Geological Society, Kraków, pp. 25–50.
Guidebook is available online at www.ing.uj.edu.pl/ims2015

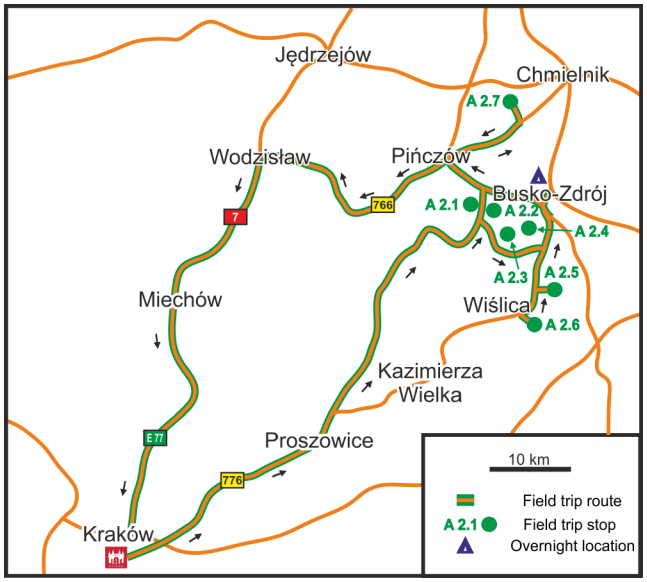

Fig. 1. Route map of field trip A2.

In Poland, the largest group of outcrops is situated in the Nida river valley in the area known as Ponidzie. These evaporites, named the Nida Gypsum deposits, and known also as the Krzyżanowice Formation, are represented by spectacular primary gypsum deposits which include selenite facies comparable to the famous Messinian selenites of the Mediterranean. The Nida Gypsum deposits are the best studied part of the Badenian sulphates in the Carpathian foredeep. Their outcrops offer an excellent insight into ancient sedimentary facies and environments of the giant-selenite dominated margin of the evaporite basin. The presentation of these unique facies is a primary aim of the field trip.

Regional geological background

The Nida Gypsum deposits are a part of the Cenozoic (Miocene) infill of the Carpathian foredeep, which at Ponidzie covers eroded Mesozoic substrate of the southern structural margin of the Holy Cross Mts. The Jurassic and Cretaceous carbonates forming this substrate were tectonically deformed and uplifted during the latest Cretaceous and Paleocene, and were subjected to intensive weathering and erosion in Paleogene and Miocene times (Fig. 3; Jarosiński *et al.*, 2009).

Then, in Badenian time (Middle Miocene, Paratethyan equivalent of late Burdigalian, Langhian and early Serravallian, Fig. 4), the Nida area was flooded with marine transgression coming from the side of the Carpathian foredeep. The biostratigraphic and sedimentologic studies suggest that the marine deposits covering the Mesozoic substrate can represent the second of the three major Badenian transgressive events in the Central Paratethys (i.e. the "major transgressive event within NN5"; Kováč *et al.*, 2007; or "the Mid-Badenian transgression"; Hohenegger *et al.*, 2014), characterized by dominant planktonic foraminiferal assemblages with

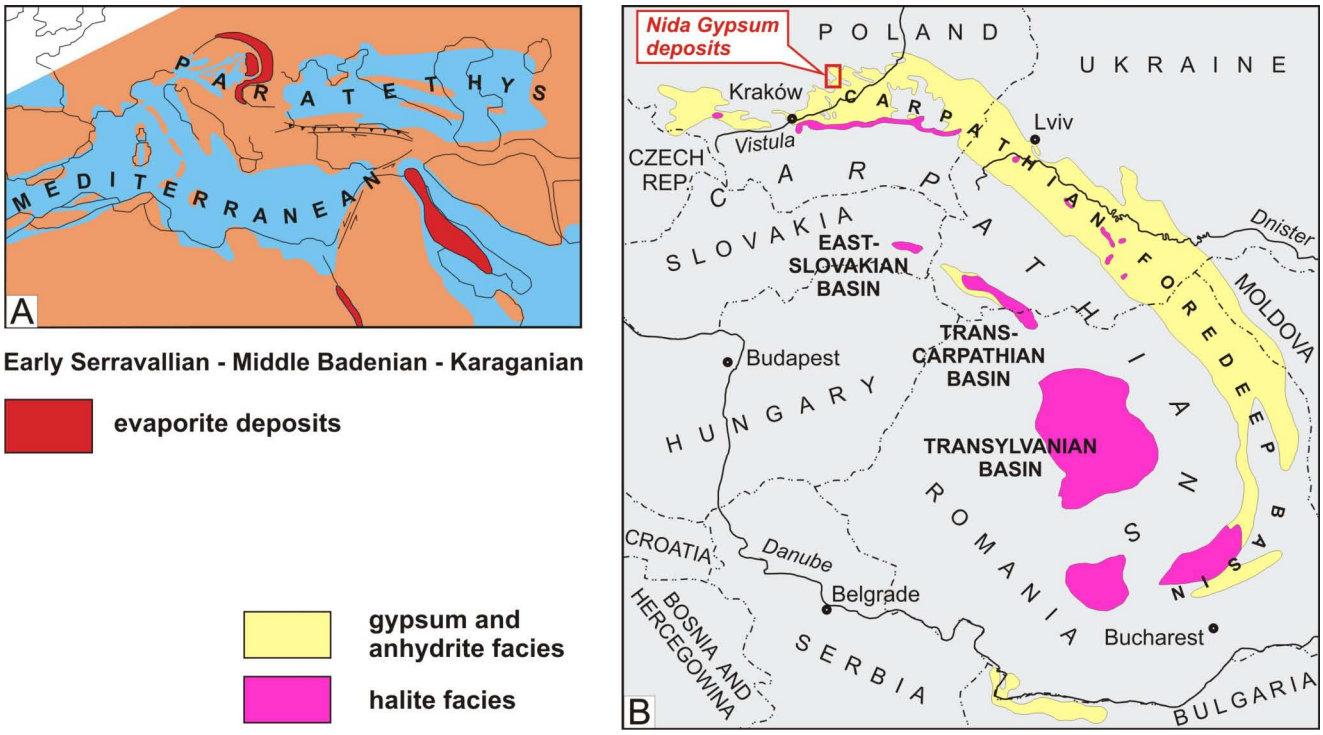

Fig. 2. Palaeogeography during the Badenian salinity crisis (**A** – after Rögl, 1999), and present-day distribution of the Badenian evaporites (**B** – after Khrushchov and Petrichenko, 1979, and other sources).

Fig. 3. Geological map of the Nida Gypsum area, without Pliocene and Quaternary cover, the carbonates enclosed within the Nida Gypsum deposits are shown in blue, after many sources cited in Bąbel (2002b), corrected after Remin (2004, Fig. 1C). Field trip stops A2.1–A2.7 shown with arrows. Broken line shows position of the cross section in Fig. 5B.

Praeorbulina glomerosa circularis (Blow) and *Orbulina suturalis* Brönnimann (Alexandrowicz, 1979; Osmólski, 1972; Dudziak and Łuczkowska, 1992; Kováč *et al.*, 2007; D. Peryt, 2013a; Paruch-Kulczycka, 2015). The deposition of the Badenian evaporites in the Ponidzie region started later and has been arrested by the next marine flooding, correlated with the last major transgressive event in the Central Paratethys, in late Badenian (Kováč *et al.*, 2007). In Ponidzie this last Badenian transgression has led to deposition of marine marls of the Pecten Beds overlying the gypsum deposits (Śliwiński *et al.*, 2012).

Miocene Central Paratethyan stratigraphy

The Neogene (Miocene) Central Paratethys was poorly connected with the ocean. Restricted faunal exchange and evolution of endemic species hamper biostratigraphic correlations between the Paratethyan and the Mediterranean deposits. The Neogene stratigraphy of the Central Parathetys is established according to the local stratigraphic scale and the deposits discussed during the field trip embrace two regional Paratethyan stages: the Badenian and the Sarmatian. The chronology of the Badenian, its subdivision into substages, and the age of the Badenian-Sarmatian boundary, are highly controversial and are a subject of the ongoing debate (Fig. 4; Kováč *et al.*, 2007; Śliwiński *et al.*, 2012; Hohenegger *et al.*, 2014; Wagreich *et al.*, 2014). In this paper we use the traditional subdivision of the Badenian in the Polish Carpathian Foredeep into the Lower, Middle and Upper Badenian, where the Middle Badenian is coeval with the time of evaporite deposition.

Chronology of the Badenian salinity crisis

Biostratigraphic and radiometric data indicate that in the Carpathian Foredeep Basin, the salinity crisis took place in the earliest part of the Neogene Nannoplankton Zone 6 (NN6: *Discoaster exilis* Zone), i.e. in the earliest Serravallian (Peryt, 1999; Garecka and Olszewska, 2011), and it lasted much less than 940 ky (Śliwiński *et al.*, 2012). Sedimentological data suggest that the crisis

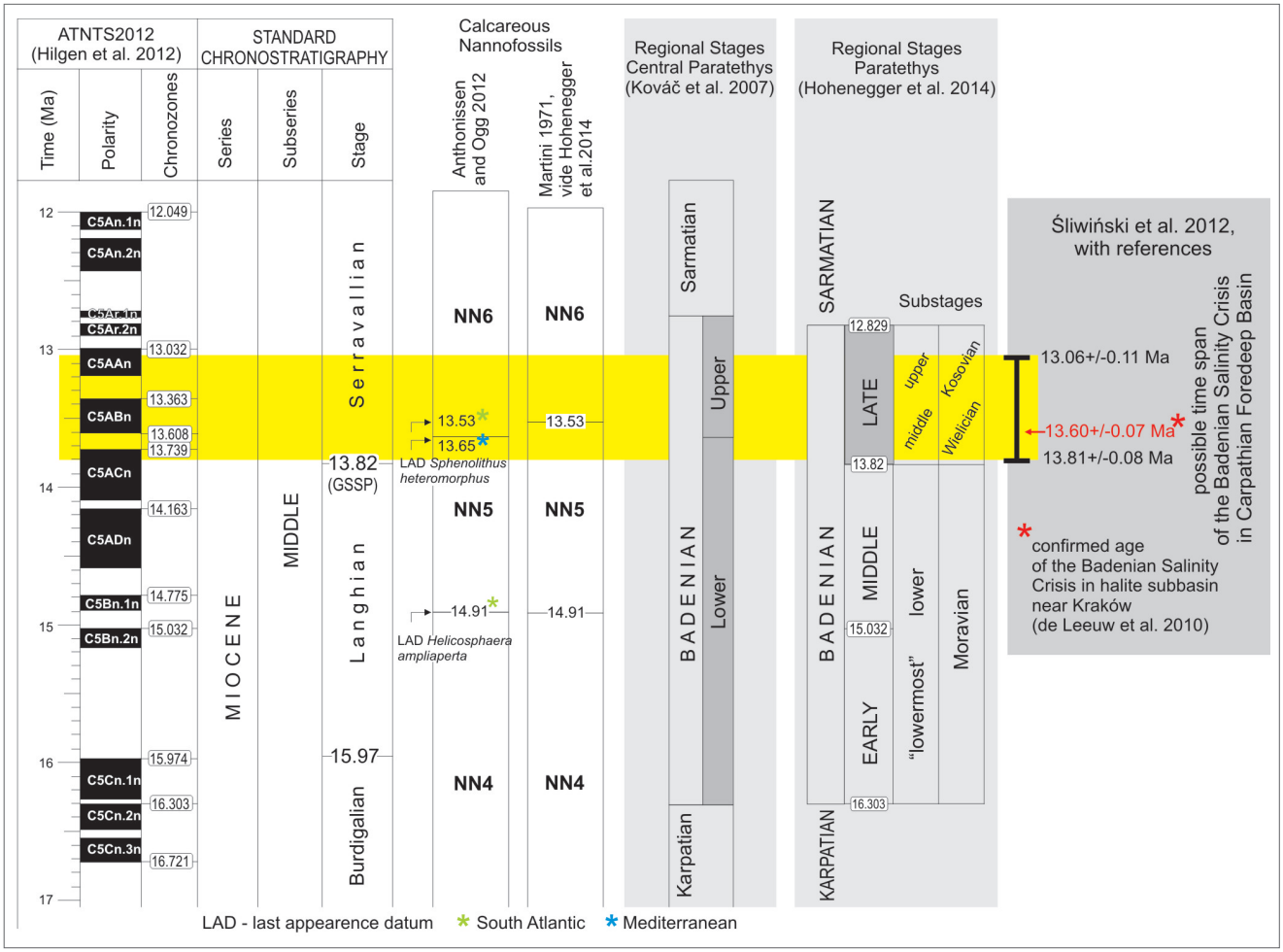

Fig. 4. Stratigraphy of the Middle Miocene regional Central Paratethys stages, according to selected current concepts, compared to the standard Mediterranean stages; chronology of the Badenian salinity crisis in the Carpathian foredeep shown in the last right column.

could be very short, only 20–40 ky in duration. According to radiometric dating of the pyroclastic deposits underlying, overlying and intercalating the evaporites in the Carpathian Foredeep, deposition of the Badenian evaporites started shortly after ca. 13.81±0.08 Ma, their deposition continued at ca. 13.60±0.07 Ma, and it ended before ca. 13.06±0.11 Ma (Fig. 4; de Leeuw *et al.*, 2010; Bukowski, 2011; Śliwiński *et al.*, 2012). The salinity crisis was apparently preceded by climate cooling correlated with the global oxygen isotope event Mi3b (de Leeuw *et al.*, 2010; Peryt and Gedl, 2010; D. Peryt 2013a).

Characteristics of the evaporites, paleogeography and model of the basin

The Carpathian Foredeep Basin is the largest Badenian evaporite basin in the Central Paratethys (Fig. 2B). The Badenian evaporites in this basin form one horizon of gypsum, anhydrite and halite deposits, up to a few tens of metres thick. The marginal gypsum deposits include extensive accumulations of selenites. The central axial areas of the basin were dominated by the laminated Ca-sulphate facies, clay and halite. This was presumably deeper zone of the basin (Fig. 5A; Kasprzyk and Ortí, 1998; Bąbel and Bogucki, 2007). The basin comprised several subbasins; halite subbasins along the axis of the foredeep and less pronounced gypsum subbasins in the northern margin of the basin, commonly considered to be a part of a giant sulphate platform or 'shelf' (Kasprzyk and Ortí, 1998). Presumed shoals and islands apparently lay in between and within the subbasins, and their position could change with time. The large area devoid of evaporite deposits, near Rzeszów, was interpreted as an island (Rzeszów Island; Figs 2B, 5A), and the area between this island and the Miechów Upland as a broad uplift or semi-emerged barrier separating sulphate and halite subbasins during deposition of the selenite facies (Becker, 2005; Bąbel and Becker, 2006; Bąbel and Bogucki, 2007). The Nida Gypsum deposits occupied the north side of this barrier, at least during the selenite deposition (Fig. 5A).

The gypsum basin was a depression without open-water connections with the seas and with the water level lowered below the global sea level due to evaporite drawdown a few tens of meters deep (Fig. 11D; Peryt, 2001, 2006; Bąbel, 2004, 2007b; D. Peryt, 2013b). Such an interpretation fits to the fact that the areal extent of the evaporites in the Carpathian Foredeep Basin is remarkably smaller than both, the under- and overlying marine Badenian deposits. This concept fits also geochemical data, and works very well for the event stratigraphic and facies analyses of the gypsum deposits (Bąbel, 2005a, b). The evaporite basin was similar to saline lakes, where water level changes independently on the global seawater level changes, and commonly more rapidly and irregularly than the sea level. Thanks to high accommodation available in such a basin, an extremely shallow water deposition could continue for a long time without any substantial erosion. The Badenian gypsum facies are indeed very similar to those recorded in modern coastal marine salinas (Kasprzyk, 1999).

The Nida Gypsum deposits

The Nida Gypsum deposits occupy the territory of three tectonic units: the Połaniec Trough, the Wójcza-Pińczów Horst, and the Solec Trough (Fig. 3). Formation of these structures is related mainly to the post-evaporitic late Badenian and to some degree to the Sarmatian and later faulting (Czarnocki, 1939; Rutkowski, 1981; Krysiak, 2000; Jarosiński *et al.*, 2009). Gypsum beds lay more or less horizontally and reach the thickness of nearly 52 m in boreholes, though this thickness was not corrected for dip. In Borków quarry, they are 37 m thick, and this is the largest thickness observed in outcrops. The sequence of the Nida Gypsum deposits is bipartite. The upper part is mostly clastic and represented by microcrystalline and fine-grained gypsum. This part of the sequence, called allochthonous, clastic or microcrystalline unit, is mostly eroded, mainly in the Quaternary. The lower part of the sequence is chiefly composed of coarse-crystalline gypsum (selenites) and is called autochthonous or selenite unit. This unit is better preserved and exposed. Anhydrite is absent and clay intercalations are quite common. In some places limestone occurs, and such limestone body at Czarkowy (6 km SSE of Wiślica) contained native sulphur exploited in the 18th through 20th centuries (Fig. 3; Osmólski, 1972).

Stratigraphy of the Badenian gypsum basin

Lithostratigraphy. The gypsum section comprises a set of thin layers showing the same characteristic features, and the same constant sequence in the northern margin of the Carpathian Foredeep Basin from the

Ponidzie region in Poland as far as environs of Horodenka in Ukraine, and also to the Czech Republic. These layers, representing the smallest-scale lithostratigraphic units, have been first recognized in the Nida area by Wala (1980, and earlier papers) who designated them by letters from a to r (Figs 5B, 7A, 8A, 9A, 12A, 17-18). The layers can be grouped into larger lithostratigraphic units recognized by Kubica (1992) in drill cores in the northern part of the Badenian basin, and designated by capital letters from A to G (Figs 5B, 17).

Event stratigraphy. Methodology of event stratigraphy applied to the Badenian gypsum deposits in the entire basin, permitted to recognize several marker beds and to connect them with isochronous basinal events (Peryt, 2001, 2006; Bąbel, 1996, 2005a). Two types of *isochronous surfaces* ("time lines" designated *A, C/D, Tb, Td, G/H, L1, F1*; Figs 5B, 17) were distinguished: *high-quality and low-quality isochronous surfaces*. The former represent short-term events not connected with dissolution and/or erosion. They are represented by dust or ash falls (*Tb, Td*) and growth zoning of selenite crystals (A). Low-quality *isochronous surfaces* are connected to basin-wide events of slowed deposition, non-deposition and/or erosion-dissolution (*C/D, G/H, L1, F1*).

Facies analysis

Facies analysis was performed using the facies definitions based on the original concept of mechanisms of deposition (Mutti and Ricci Lucchi, 1975). In the case of *in situ* grown selenites, the crucial depositional mechanism was syntaxial bottom-growth of crystals. Basing on the main mechanisms of deposition, several facies and subfacies can be distinguished in the Nida Gypsum deposits (which comprise gypsum, clay and carbonate sediments, Tab 1). Only the facies presented during the field trip are described below.

Giant gypsum intergrowths. *Description:* This facies is composed of large crystals (up to 3.5 m long), commonly arranged vertically and forming intergrowths similar to the $\bar{1}01$ twins. The facies does not exhibit layering except for rare dissolution surfaces. Two subfacies are distinguished according to crystal arrangement: the giant intergrowths with palisade and with non-palisade structure. Within the palisade intergrowths, two subordinate subfacies, showing different crystal structures are recognized: the skeletal and the massive intergrowths. The rare clay subfacies is built of isolated intergrowths and their aggregates (<0.5 m in size) placed in black laminated clay.

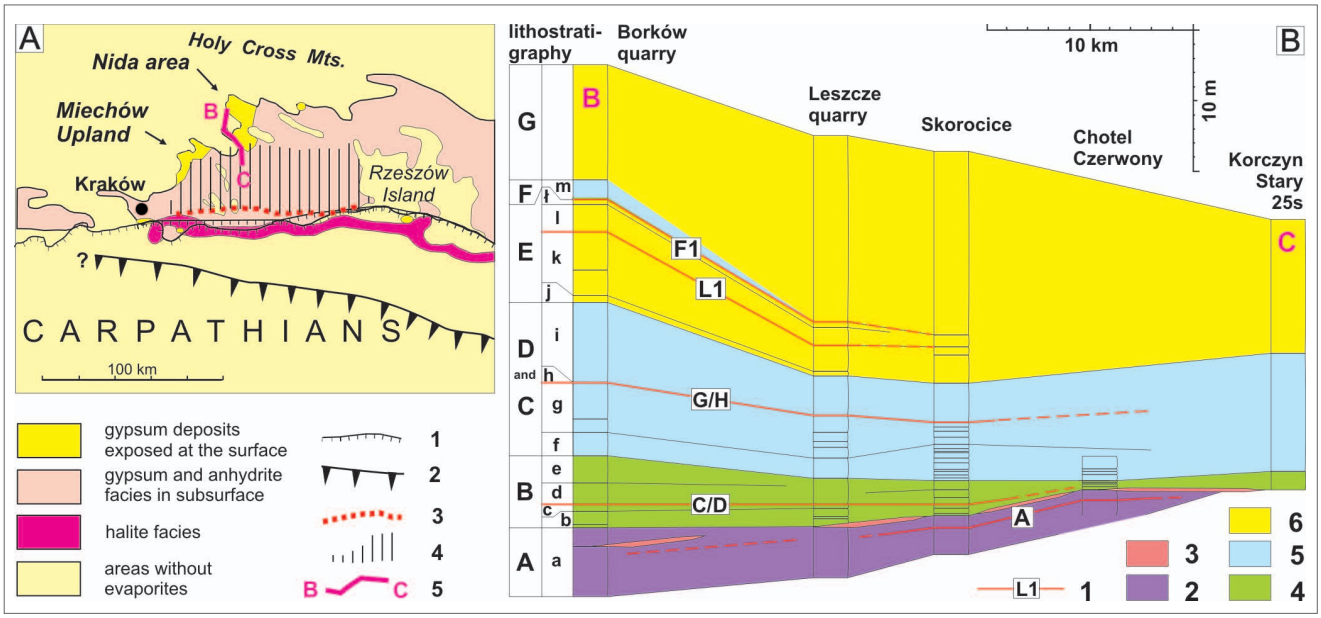

Fig. 5. Palaeogeography of the Badenian evaporite and gypsum basin. **A**) Distribution and palaeogeography of Badenian evaporites in Carpathian Foredeep Basin, 1 – main overthrusts – present-day outer boundary of the Carpathians, 2 – supposed position of the outer boundary of the Carpathians during evaporite deposition, after Ślączka and Kolasa (1997), 3–4 – paleogeographical units (Rzeszów Island is described on the map); 3 – barrier between sulphate and halite subbasins, after Połtowicz (1993), 4 – Miechów-Rzeszów barrier or shoal interpreted by Bąbel and Becker (2006), 5 – cross section shown in B; **B**) stratigraphic cross section of the Nida Gypsum deposits (see Fig. 3 for detailed location of the cross-section); 1 – isochronous surfaces, 2–6 – gypsum facies; 2 – giant intergrowths, 3 – selenite debris, 4 – grass-like facies, 5 – sabre facies, 6 – microcrystalline facies, distribution of facies after Bąbel and Olszewska-Nejbert (2012), simplified; section of the Korczyn Stary 25s borehole after Osmólski (1972).

Interpretation: This facies was created almost exclusively by upward bottom growth of gypsum crystals permanently covered with Ca-sulphate saturated brine (Bąbel, 2007b; see also Fig. 11E). The coarsest crystals, especially those lacking dissolution features, grew in the deepest zones of perennial saline pans, below an average pycnocline, at a depth not accessible to meteoric water. Because of low supersaturation, and/or organic compounds inhibiting the crystallization, gypsum nucleation was sparse and the crystal growth was mostly syntaxial. The protracted period of upward growth led to formation of extraordinarily large crystals. In the clay subfacies, this growth was accompanied by simultaneous clay deposition.

Selenite debris. *Description:* The debris is a mixture of clay and broken, abraded and dissolved crystals, up to 0.5 m long. The debris fills depressions between apices of intergrowths which are flattened by dissolution. The debris is overlain by the grass-like gypsum subfacies with clay intercalations. The deeper depressions contain small aggregates of lenticular crystals grown in situ within clay.

Interpretation: The debris is a kind of regolith and is a product of emersion and destruction of the original palisade selenite crusts by atmospheric agents and by weathering in a coastal "sabkha-like" flat, periodically flooded with meteoric waters loaded with clay. The debris accumulated in the coastal zones of the shrinking saline pans, with fluctuating water level.

Grass-like gypsum. *Description:* This facies is characterized by thin layering (<25 cm) and grass-like structures usually formed by a single generation of bottom-grown gypsum crystals. They create crusts 0.1–20 cm thick, intercalated with layers of fine-grained gypsum and/or clay. Larger grass-like crystals are similar in morphology to the giant intergrowths. The grass-like facies encloses four subfacies: (I) with crystal rows, (II) with stromatolitic domes, (III) with clay intercalations, and (IV) with alabaster beds.

Interpretation: This facies was deposited by two alternately acting main mechanisms: (I) syntaxial bottom-growth of large crystals, and (II) microbialite, clastic, or pedogenic gypsum deposition. The facies was formed in shallow periodically emerged saline pans or flats. The thickest selenite crusts intercalated with fine-grained gypsum were deposited at a depth that could be only occasionally reached by meteoric water and represent relatively deeper brines. The thinnest selenite crusts (<5 cm) intercalated fine-grained gypsum represent ephemeral saline pans passing into evaporite shoals.

Gypsum microbialites (gypsified microbial mats). *Description:* The facies is represented by layers of fine-crystalline gypsum showing wavy crenulated lamination and fenestral structures filled with coarse-crystalline gypsum cement transparent-to-honey in colour which is due to included organic matter. Such deposits commonly form thin intercalations within the grass-like facies and they appear in the layers *c* and *m1*. The lamination laterally disappears (commonly in layer c) and the facies passes into homogeneous or slightly nodular alabaster.

Interpretation: The layers represent gypsified microbial mats. They were deposited on a semi-emerged evaporite shoal at the margins of ephemeral to shallow perennial saline pans. The presence of such pans is recorded by thin grass-like selenite crusts, intercalated with gypsum microbialite deposits. Alabaster deposits associated with gypsified microbial mats are interpreted as pedogenic sediments formed during emersion of evaporite shoals, or as deposits of thin brine sheets.

Sabre gypsum. *Description:* This facies is characterized by curved ("sabre") crystals (10-95 cm long; Fig. 5B, C) and thick bedding (0.2-1.5 m). The crystals started to grow vertically and then curved laterally due to crystal lattice twisting. Minute *100* twins are commonly 'nuclei' of sabre crystals. A characteristic feature of this facies is concordant orientation of crystal apices traceable over long distances and presumably reflecting the direction of bottom brine currents. Locally, a few meters high and >10 m wide domal structures occur. The sabre gypsum encloses: flat bedded subfacies, entirely built of bottom-grown crystals, and wavy bedded subfacies, with bottom-grown crystals scattered within flat-to-wavy laminated fine-grained gypsum commonly showing microbialite domal structures. Selenite nucleation cones are common in this facies.

Interpretation: The flat bedded subfacies was created by syntaxial bottom growth of crystals associated with frequent formation of new individuals. The new crystals accreted on surfaces of older ones, especially on their upper faces. This subfacies was deposited in brine more than 1 m deep. Such a depth was necessary for existence of permanent density stratification maintaining bottom growth of large crystals and giant domes, which are

primary forms. This growth was disturbed by refreshments, connected with the drop of the pycnocline in a perennial saline pan, recorded by dissolution surfaces, and microbial gypsum deposition which indicate a relatively shallow depth. The wavy bedded subfacies were deposited in a similar environment, but are associated with both, mechanical and microbialitic deposition of fine-grained gypsum. The fine-grained gypsum remained mostly uncemented and soft and it was subjected to deformations, which included both compactional deformations and gravity creep and slumps. Intercalations of debris flow deposits are noted in this facies.

Selenite debris flow. *Description:* This facies consists of broken, abraded and/or dissolved gypsum crystals scattered within a matrix of fine-grained gypsum. The clasts, mostly fragments of elongated sabre-like crystals, commonly show horizontal orientation. The facies appears in layers, up to >1 m thick, associated with microcrystalline and sabre gypsum facies.

Interpretation: The fabric of this facies and the occurrence of fine-grained matrix between the crystal clasts suggest a debris-flow transport mechanism, although local grain-flow cannot be excluded. Selenite clasts could derive from the wavy bedded sabre facies and originally could crystallize on basin slopes as loose aggregates, possibly within microbial mats or soft microbialite deposits. These selenites were then redeposited from there into deeper zones of saline pans as slumps and debris flows. Crystal fragmentation and abrasion took place during redeposition.

Microcrystalline gypsum. *Description:* This facies includes many lithologic varieties (subfacies) which are built of macroscopically invisible crystals. The most widespread subfacies are thin laminated gypsum (with laminae commonly less than 1 mm thick), alabasters or compact gypsum, and breccias. Traces of bottom-grown halite crystals (<1 cm in size) are present in some beds, as well as evidence of their synsedimentary dissolution both on the surface and within soft gypsum mud (Kwiatkowski, 1972). Slump and soft-sediment deformation structures are very common. This facies locally contains thick clay intercalations.

Interpretation: The microcrystalline facies represents a subaqueous environment of a brackish-to-saline pan (with fluctuating salinity), dominated by allochthonous clastic deposition. The laminated gypsum was deposited by fallout of gypsum grains from suspension clouds. Lamination and extremely small grain sizes suggest a calm environment, though the presence of rare wash-out surfaces and ripples indicates episodic action of strong bottom currents. Each lamina may represent one flood of run-off meteoric waters which swept out gypsum detritus from emerged coastal flats composed of earlier deposited gypsum sediments exposed to weathering (Kasprzyk, 1999). Lack of bottom-grown gypsum crystals and common soft-sediment deformations prove that gypsum crystallized neither within sediment nor at the sediment-water interface. Contrary to gypsum, halite crystallized directly at the bottom, indicating that the brine was saturated with NaCl at least temporarily.

Sedimentary environment

The distinguished facies, which correspond to the lithostratigraphic units, represent various environments (from subaqueous and more or less shallow-brine to subaerial) of a giant salina-type basin. The gypsum layers, particularly in the autochthonous unit, originated in a vast flat-bottom zone of the basin. This area was occupied by a system of variable perennial saline pans (<5–20 m deep, dominated by selenite deposition) and evaporite shoals (dominated by gypsum microbialite deposition). The various morphologies and fabric of the bottom-grown crystals in the giant intergrowths and sabre gypsum facies, reflect different compositions and properties of the brine in the separate saline pans evolving in time.

The layer-cake architecture of the gypsum facies visible in the autochthonous unit, suggests that the basin was infilled with evaporite deposits by vertical accretion (aggradation). Aggradational deposition was controlled by water or brine level fluctuations within the basin or subbasins (Bąbel, 2007b). Because the basin was separated from the sea by some emerged barriers (Fig. 11E), these fluctuations were only weakly dependent on sea level changes but were rather controlled by regional climate.

History of sedimentation

Integration of facies analysis and event stratigraphic studies allowed reconstruction of the sedimentary history of the gypsum basin. After initial evaporite drawdown, the northern margin of the basin evolved from a large perennial saline pan (with deposition of the giant

gypsum intergrowths) into an evaporite shoal (with grass-like gypsum deposition) and then back again into a perennial pan (with sedimentation of the sabre gypsum). Later, deposition of clastic gypsum prevailed. It was due to a dramatic change in salinity and chemistry of the water. This deposition was interrupted by a short return to selenite deposition recorded in the northern part of the evaporite basin by a thin bed of grass-like and sabre gypsum (unit F in Figs 5B, 17). This event was preceded by an inflow of marine water to the basin, documented by foraminifers present in the underlying clays (D. Peryt, 2013b). Evaporite deposition was arrested by a flood of marine waters and rapid deepening.

Paleogeography

The distribution of the facies and the other data suggest that the relief of the Nida Gypsum basin raised slightly towards the south, towards the centre of the evaporite basin, especially during the deposition of the lower selenite unit. It was suggested that the broad morphological barrier elongated W-E separated the gypsum depositional area in the north from the halite-dominated zone and the halite subbasins in the south (Fig. 5; Bąbel, 2005b; Bąbel and Becker, 2006; Bąbel and Bogucki, 2007) and the Nida Gypsum deposits (particularly the selenite unit) formed on a broad northern margin of this barrier.

Badenian and Messinian selenite cycles

The vertical pattern of the Badenian selenite facies: giant intergrowths → grass-like gypsum → sabre gypsum, is similar to the Messinian selenitic cycle: massive selenites → bedded selenites → branching selenites, and both patterns were interpreted in nearly the same way, i.e. as large-scale fluctuations of the water level, namely highstand-lowstand-highstand cycle, in the basin with a drawdown water level (Kasprzyk, 1993a; Bąbel, 2005b, 2007b; Lugli *et al.*, 2010). The Badenian lowstand-highstand transition is associated with the rising trend in Sr content of the selenite crystals and therefore it was interpreted as having a character of deepening-upwards and also brining-upwards (Kasprzyk, 1994, 1999; Rosell *et al.*, 1998; Bąbel 2004, 2007b). This transition was also interpreted as the "autogenetic" or "autocyclic" transgression characteristic of the post-drawdown phase in evaporite basins (Rouchy and Caruso, 2006; Warren, 2006). The Messinian cycles were interpreted as driven by cyclic climatic changes (i.e. periodic transitions: wet climate – arid climate – wet climate) related to precessional changes in the position of Earth orbit, and according to this interpretation the selenite cycles record the time span of ca. 21 k.y. typical of the precessional cycles. Such time of deposition fits to the Badenian lower selenite unit as well.

Stop descriptions

A2.1 Gacki, pre-evaporite Badenian marls and basal part of the Nida Gypsum succession with the largest giant crystal

Leaders: Maciej Bąbel, Krzysztof Nejbert, Danuta Olszewska-Nejbert

A vast abandoned gypsum quarry at Gacki turned to undeveloped recreation area with some ponds (Fig. 6). The NE wall of the road cut at the entry is a protected exposure presenting pre-evaporite Badenian marls and basal selenite part of the Nida Gypsum succession, giant crystal intergrowths up to 3.5 m long, sabre gypsum facies, selenite nucleation cones, and evidence of post-evaporite tectonics. (50°27′15″ N, 20°35′18″ E)

The Badenian deposits are cut by a vertical fault, with a throw of ca. 13 m. Its east uplifted side is composed of the early Badenian marine marls underlying the giant intergrowths layer forming the top of the hill. The marls are >15 m thick, and lay on eroded surface of Cretaceous (Campanian) marls, once exposed 300-350 m SE, at the foot of the slope. The visible part of the Badenian marls contains glauconite, pyroclastic intercalations, mollusks – pectinids, the oyster *Neopycnodonte cochlear* (Poli) – and foraminifers characteristic of the regional biostratigraphic zone *Uvigerina costai*. Below these marls, which are ca. 10 m thick, the older *Orbulina suturalis* (=*Candorbulina universa*) zone was documented (Łuczkowska, 1974). The lower part of the marls represents the standard Neogene Nannoplankton Zone 5 (NN5, *Sphenolithus heteromorphus* Zone), and the marls above, directly underlying the gypsum may represent NN6 zone (Dudziak and Łuczkowska, 1992). The fossils indicate that marine sedimentation preceded the evaporite deposition.

The giant intergrowths attract attention by exceptionally large sizes of crystals which in this area are particu-

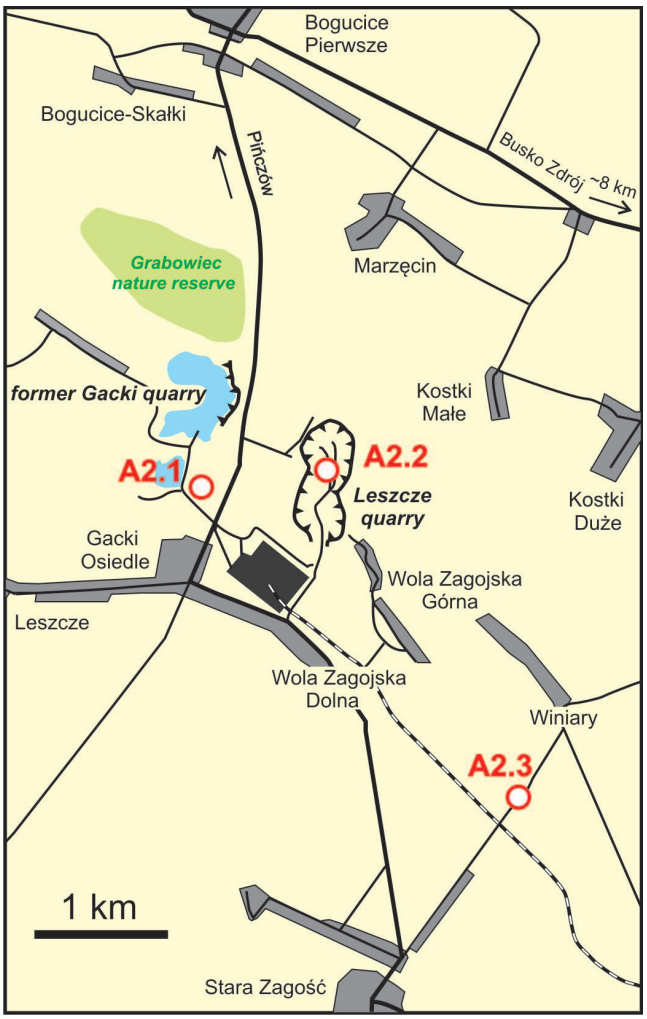

Fig. 6. Detailed location of the field trip stops Gacki (A2.1), Leszcze (A2.2) and Zagość-Winiary (A2.3).

larly large. The spectacular palisade of 1–2 m long crystals is seen high in the wall of the outcrop. One crystal attains the record size among the giant intergrowths and the minerals of Poland. The specimen is 3.2 m in length. It is partly destroyed and can be estimated as originally 3.5 long (Fig. 7A, B). This crystal is one of the two largest so far documented in Poland and still preserved natural crystals. The other crystal of the same estimated sizes is exposed in the outcrop of the giant intergrowths in nearby Bogucice-Skałki (Fig. 6; Bąbel, 2002a). The giant intergrowths are a crystallographic curiosity recognized so far only in the Carpathian Foredeep. Although similar to the contact $\bar{1}01$ gypsum twins, the intergrowths differ from any twins in lacking crystallographic symmetry between component crystals (Fig. 8C, D). The other uncommon feature is the primarily skeletal structure of the giant crystals.

The sabre gypsum facies is exposed in the west downthrown side of the fault. The sabre crystals show apices turned in similar azimuths (to N and E), which is interpreted as a paleocurrent indicator (apices are oriented upstream, see Stop A2.4). The nucleation cone structures formed by synsedimentary load deformation generated by the crystals growing on the soft substrate are present in layer *h*, and also at the base of the giant intergrowths (Fig. 7A, B).

References to stop A2.1: Alexandrowicz (1967), Alexandrowicz and Parachoniak (1956), Bąbel (1986, 1987, 1991a), Bąbel *et al.* (2010, 2013, with references), Dudek and Bukowski (2004), Dudziak and Łuczkowska (1992), Łuczkowska (1974), Osmólski *et al.* (1978).

Fig. 7. Outcrop at Gacki. **A)** View of the outcrop, the giant crystals are outlined, **B)** the largest gypsum crystal (after Bąbel *et al.*, 2010, modified), **C)** selenite nucleation cones formed by sabre crystals.

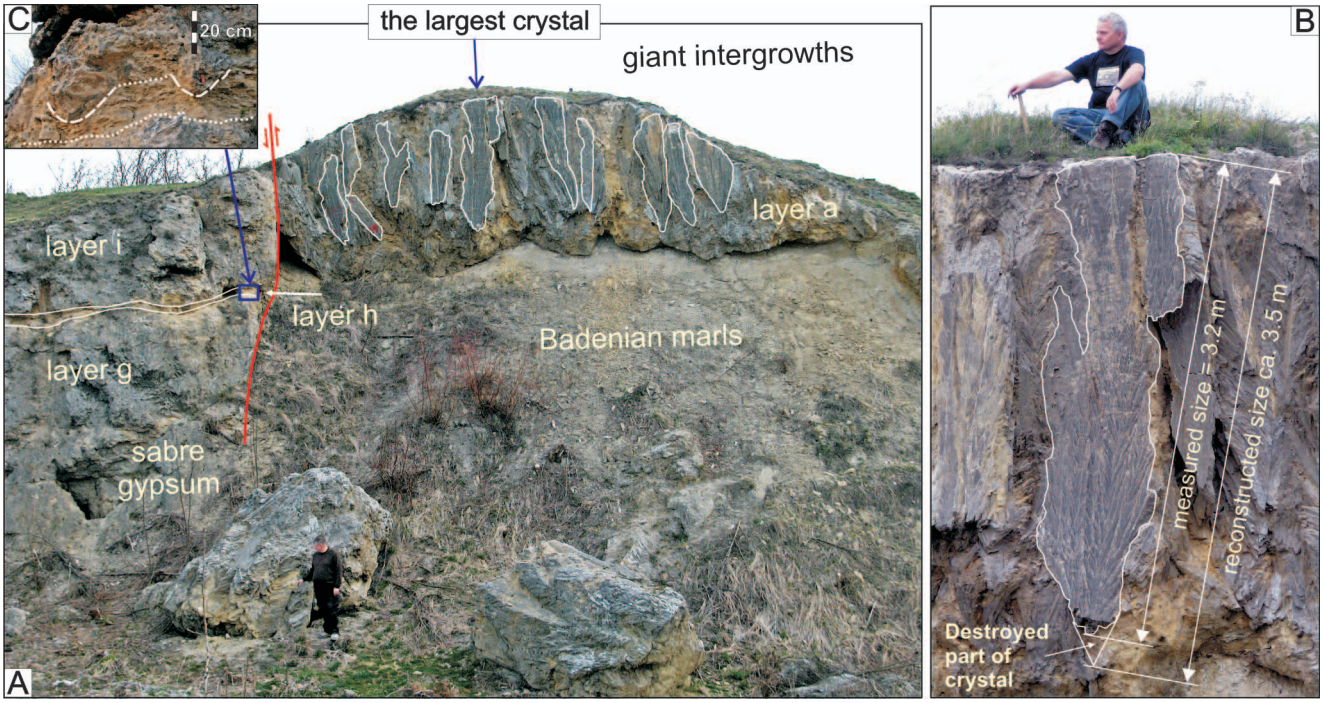

A2.2 The Nida Gypsum deposits in the Leszcze quarry

Leaders: Maciej Bąbel, Danuta Olszewska-Nejbert, Krzysztof Nejbert, Damian Ługowski, Teresa Lisek[1]

[1]ZG Kopalnia Gipsu "Leszcze" S.A
(teresa.lisek@dolina-nidy.com.pl)

This is a great active quarry (Fig. 6). Visits only by permission from the management. (Entrance to the quarry: 50°26′ 59″ N, 20°36′09″ E)

We observe here the typical facies range of the Nida Gypsum succession, with giant intergrowths showing skeletal structures, grass-like gypsum with clay intercalations, gypsum microbialitic structures, sabre gypsum, clastic microcrystalline and laminated gypsum, traces after halite-solution, and gypsum breccias and megabreccias related to halite-solution collapse and subsidence.

The pre-evaporite Badenian marls exposed in the quarry, underlying the giant intergrowths layer similarly as in stop A2.1, represent biostratigraphic zone *Uvigerina costai*, recognized here in the sampled 1.6 m interval below gypsum (D. Peryt, 2013a). The delphinid vertebra found in these deposits (Czyżewska and Radwański, 1991) confirm that marine deposition preceded the onset of evaporation.

The selenite unit is exposed in the lower exploitation level. The giant intergrowths represent palisade and skeletal forms, most probably typical of the deeper, less oxygenated brine (Fig. 8A, B). Higher up the section the microbialite structures are common in layer *e*, within the grass-like gypsum facies with clay intercalations. This subfacies represents a semi-emerged coastal evaporite shoal, covered with microbial mats and seasonally overflooded with clay-loaded meteoric waters transported by sheet floods. Further up the section the typical sabre facies is exposed, representing the same beds as in stop A2.1.

The 12–15 m thick clastic unit is exposed in the upper exploitation level. Laminated gypsum common in this interval contains traces of dissolved (<1 cm) halite cubes, which grew in situ at the bottom of the basin. In places, thin beds of residual gypsum ("alabaster") left after halite dissolution are present. Soft-sediment deformations, mostly folds and slump structures, as well as deformations related to synsedimentary and early diagenetic halite solution, commonly appear in some beds. There are also larger-scale deformations which involve the entire thickness of the clastic unit. Nearly the whole ca. 500 m long wall of the quarry is built of megabreccia with blocks up to 10 m and more in size, showing the features of in situ crushing (Fig. 8E, F). This megabreccia passes laterally into regularly bedded deposits seen currently in NW part of the quarry. Laminated gypsum forms the so-called "breccias without matrix" and is a component of the breccias with alabaster matrix. The former commonly forms vertically elongated bodies typical of the infillings of collapse chimneys (Fig. 8E, F). Various bodies of homogeneous alabaster are present and resemble clastic dykes. In many places such thin dykes run parallel to lamination. The structure of the wall is additionally complicated by veins or pockets of karst breccia in which rounded gypsum components are placed within gypsiferous dark clay. Various fault surfaces with slickensides are recorded but without druse-like gypsum mineralization, indicating that deformation took place in the soft unconsolidated or poorly consolidated rocks. The base of the brecciated zone is formed by a flat top surface of the selenite unit (top of layer *i*) and the breccia does not show any connections with the faults cutting the underlying layers *a-i*. The origin of these megabreccias, exposed in the quarry for a long time (Bąbel, 1991b, pl. 15, fig. 2; Bąbel, 1999b, pl. 4, fig. 1 and pl. 5), is related to large scale postdepositional solution of halite originally present in the lower part of the clastic unit. The breccias were formed by fracturing and gravitational collapse of sediments over the zones of dissolving halite.

At Leszcze, the gypsum deposits are covered with Miocene marls containing foraminifers, thin-walled mollusks, pteropods (planktonic gastropods, very common), and echinoids (M. Bąbel, unpubl. data). These fossils indicate a marine environment of normal salinity characteristic of the late Badenian transgression following the Badenian evaporite event. Coeval marls in nearby Winiary (Fig. 6; Urbaniak, 1985) contained abundant pteropods *Limacina* (="*Spiratella*") together with the endemic pectinid *Palliolum bittneri* (Toula, 1899), (=*Chlamys elini Zhizhchenko*, 1953), which both are typical of the Upper Badenian Pecten Beds (Śliwiński *et al*., 2012).

References to stop A2.2: Bąbel (1987; 1991a, b), Czyżewska and Radwański (1991); Kwiatkowski (1972); D. Peryt (2013a).

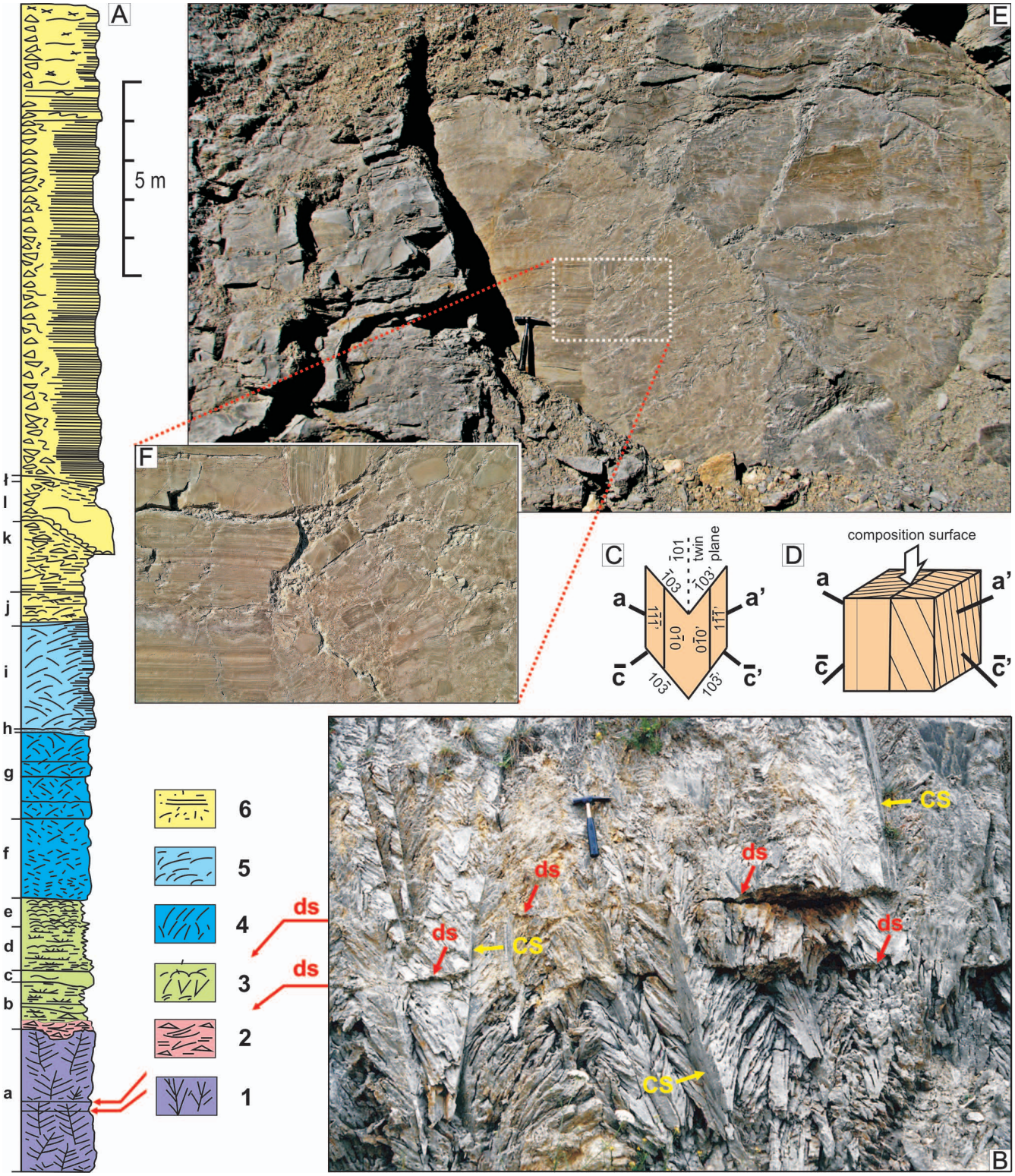

Fig. 8. Leszcze quarry. **A**) Section of the gypsum deposits, layers lettered after Wala (1980). Facies: 1 – giant gypsum intergrowths, 2 – selenite debris, 3 – grass-like gypsum, 4 – flat-bedded sabre gypsum, 5 – wavy-bedded sabre gypsum, 6 – microcrystalline gypsum. **B**) Giant gypsum intergrowths with palisade and skeletal structure, *ds* – dissolution surfaces, *cs* – composition surface of the intergrowth, **C**) orientation of gypsum crystals in the exemplary $\bar{1}01$ twin, **D**) typical orientation of gypsum crystals in the intergrowths, hachure marks the position of *010* cleavage planes, **E**) megabreccia built of microcrystalline gypsum, **F**) detail of E with "breccias without matrix" on the right.

A2.3 Zagość-Winiary road-cut across the gypsum cuesta, gypsum sequence with reduced thickness on Cretaceous substrate

Leaders: Maciej Bąbel, Krzysztof Nejbert, Damian Ługowski, Danuta Olszewska-Nejbert

Artificial exposures on both sides of the road deeply entrenched into a steep erosional escarpment formed on the Nida Gypsum (Fig. 6). (50°25′58″ N, 20°37′29″ E)

We can see here Badenian evaporites overlying almost directly their Cretaceous substrate, a reduced section of the gypum succession, massive and non-palisade giant intergrowths subfacies, grass-like gypsum with clay intercalations, the sabre and the selenite debris-flow facies.

The gypsum deposits in this outcrop show dip of ca. 30°N and lie with the angular unconformity of ca. 40° almost directly on eroded Cretaceous substrate (Fig. 9). This substrate is built of Campanian marls and siliceous chalks (opokas) which contain remains of echinoids (*Echinocorys* sp.), inoceramids, ammonites (*Baculites* sp. and others) and belemnites. In the contact zone with the gypsum, the marls are brecciated and fractured and reveal shallow pockets filled with limonitic brecciated clay and numerous angular mud clasts (Fig. 9C). These deposits are covered with 1-3 cm thick discontinuous limestone layer, containing glauconite grains. The marls with brecciated clays are interpreted as remnants of pre-evaporite weathered zone developed on the surface of the Coniacian marls after their emersion. The limestone with glauconite probably represents Badenian marine deposits. Similar deposits are known from the described region (Alexandrowicz, 1967; Osmólski, 1972; Oszczypko and Tomaś, 1977; Krysiak, 2000).

The gypsum deposits directly overlying the Cretaceous substrate are commonly met at environs of Wiślica (Fig. 3; Czarnocki, 1939; Osmólski, 1972) and on the Miechów Upland (Becker, 2005, fig. 4). Close to stop A2.3, the early Badenian marine deposits underlying the evaporites are present and attain relatively large thickness, e.g. >15 m at Gacki (stop A2.1), 26 m at nearby Kobylniki (Fig. 13; Łyczewska, 1972), and up to 115 m at Młyny in the north (Fig. 3). The lack of such thick early Badenian marine deposits in the outcrop can be explained by non-deposition on the submarine uplift or emerged island, and existence of such paleouplifts and islands is known from the described area.

The giant intergrowths layer is ca. 1 m smaller in thickness than in neighboring outcrops (Stops A2.1 and A2.2), and the average crystal sizes in it are also smaller. Both palisade and non-palisade subfacies are present and they display rather massive structure characteristic of the shallow, well oxygenated brine (Fig. 9A, B). An unordered structure and smaller sizes of the crystals can be connected with a relatively shallower environment, closer to the coastline, and similar features were recorded in the Messinian San Miguel de Salinas basin in Spain (Rosell *et al.*, 1998).

The section above is reduced in thickness and is comparable to the section from the nearby Leszcze quarry (stop A2.2). The marker bed *c* is missing in the described section. Higher in the section the sabre facies with crystals predominantly oriented to N is present, and this orientation reflects the direction of the brine flow (see stop A2.4).

The sabre gypsum is covered with beds of selenite debris-flow ca. 2.3 m thick (Fig. 9D, E). The fragments of sabre crystals and their aggregates are common components of these beds and suggest that it was the wavy-bedded sabre gypsum facies which was destroyed in the shallower zones of the basin, and subjected to redeposition (Bąbel, 2005b). Similar redeposited selenite deposits were previously recorded in this area by Niemczyk (2005, and his earlier papers).

A2.4 Siesławice – sabre gypsum facies

Leader: Maciej Bąbel

Abandoned roadside gypsum quarries at Siesławice, slightly depressed beneath their surroundings (Fig. 10). Visible are: sabre gypsum facies with conformably oriented crystals, a selenite domal structure formed over a sunken drift tree. (50° 26′60″ N, 20° 41′31″ E)

Both the flat-bedded and the wavy-bedded sabre subfacies are seen in this outcrop, with common synsedimentary dissolution (and erosion) surfaces and compaction breaks of the crystals (Figs 11, 12). A rare sedimentary structure is seen in the lower part of layer *i*. The two empty cylinder-shaped holes are surrounded by radially grown gypsum crystals which create a kind of a domal structure over these holes (Fig. 12A, B). The holes

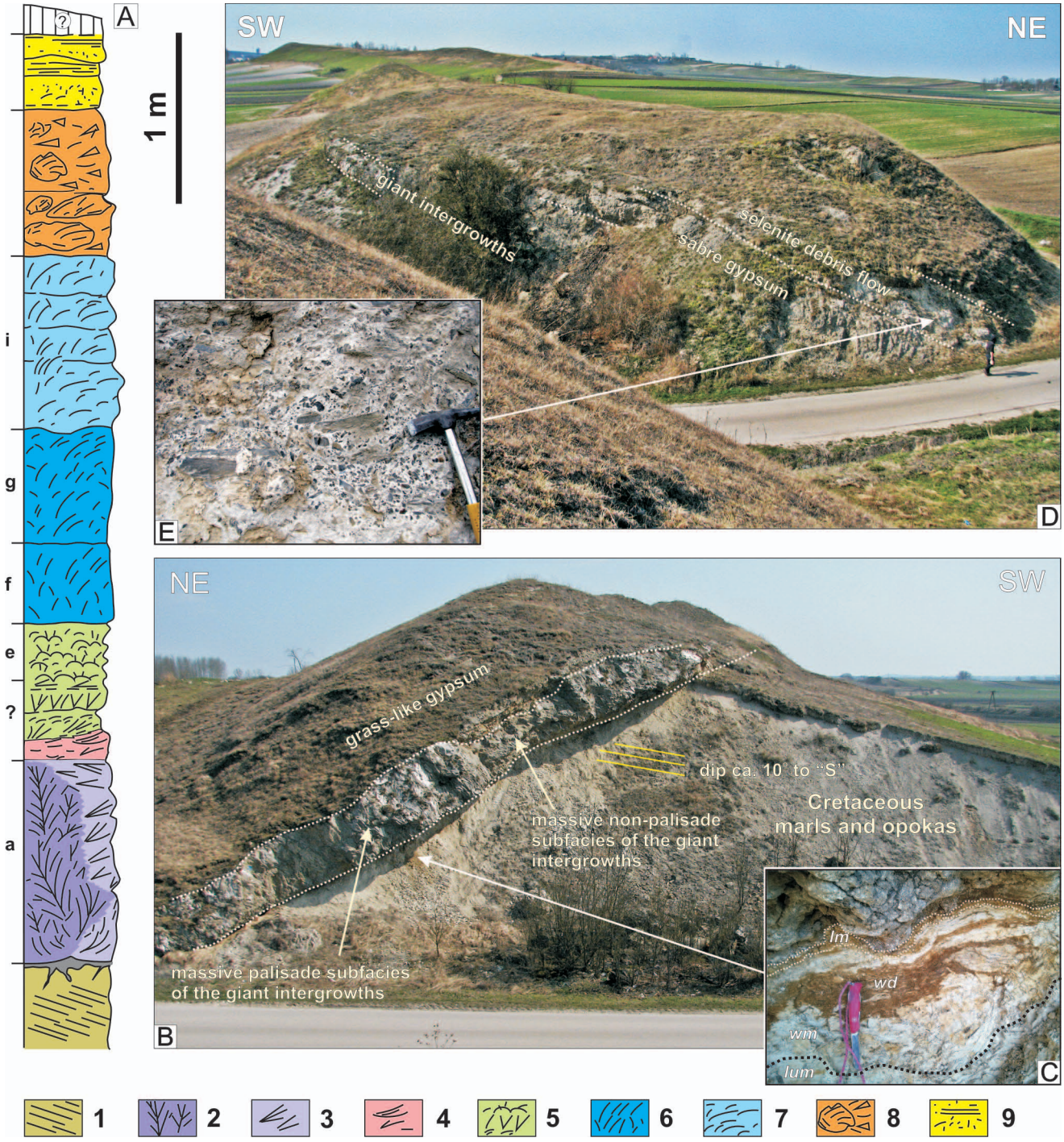

Fig. 9. Outcrop at Zagość-Winiary roadcut. **A)** Section of the gypsum cuest: a, e, f, g, i – layers after Wala (1980); 1 – marls and opokas (Cretaceous, Campanian); 2–9 – gypsum deposits (Miocene, Badenian); facies: 2 – palisade giant intergrowths, 3 – non-palisade giant intergrowths, 4 – selenite debris, 5 – grass-like gypsum with clay intercalations and stromatolitic structures, 6 – flat-bedded sabre gypsum, 7 – wavy-bedded sabre gypsum, 8 – selenite debris-flow, 9 – clastic and laminated gypsum; **B)** section of the gypsum cuesta in eastern scarp, **C)** details of the boundary between marls and gypsum, *lm* – limestone, *wd* – weathered clastic material (remnants of regolith?), *wm* – weathered marls, *lum* – less weathered and unweathered marls, **D)** hill west of the road, **E)** details of selenite debris-flow.

were formerly occupied by a tree trunk (the larger hole) and possibly its branch (the smaller hole). The tree was carried to this place from the land as a drift wood which sunk or was anchored there at the bottom, and became a substrate for the growth of gypsum crystals (Fig. 12C, D). The wood was later degraded during diagenesis. Moulds of tree trunks overgrown with gypsum crystals were found also in Borków quarry (Bąbel, 2007a, fig. 1).

The sabre gypsum facies in this outcrop shows apices of the curved crystals pointing in similar directions (to NE; Figs 11A-C, 12A), which is interpreted as a paleocurrent indicator (apices oriented upstream). The ordered

Fig. 10. Detailed location of the field trip stop A2.4, Siesławice.

orientation of the sabre crystals can be explained by competitive growth, influenced by unidirectional flow of Ca-sulphate saturated brine over the bottom (Fig. 11E). The crystals commonly started to grow from *100* twinned seeds attached to the substrate (Fig. 11F, G) and it was the earliest selection which eliminated the unfavorably oriented crystals (b in Fig. 11G) from the further growth. The sabre crystals developed from favorably oriented nuclei (*d-e* in Fig. 11G) and the specific feature of such crystals was that they grew by advance of the *120* prism faces in apical zone whereas the growth of side faces was extremely inhibited (Fig. 11F). Very regular growth zones of these faces seen on *010* cleavage surfaces suggest monomictic hydrography of the basin (Fig. 11D, E). During the further growth the sabre crystals with the apices (*120* prism faces) oriented favorably upstream grew at an accelerated rate and could survive the competition, and finally attained larger sizes then their less favorably oriented neighbours. Curved shape of the crystals is related to crystal lattice twisting which is a primary feature originating during crystal growth. The twisting of the crystal lattice finally eliminated the sabre crystal from further growth when its apex gradually became turned horizontally.

The conformable orientation of sabre crystals is a regional feature (see Stops A2.1, A2.2, A.2.3, A2.7) which indicates that the brine was flowing *en mass* generally along the coastline of the basin in the counterclockwise direction (Bąbel, 2002b). Presumably the oriented sabre crystals in the Nida area reflect only a fragment of the cyclonic longshore circulation of brine recorded in the entire basin (Bąbel and Becker, 2006; Bąbel and Bogucki, 2007). For more on this site see Bąbel (1996).

A2.5 Chotel Czerwony-Zagórze, giant intergrowths with selenite regolith covered with grass-like gypsum

Leader: Maciej Bąbel

Abandoned stone pits in Góry Wschodnie floristic nature reserve, and in its eastern margin, at Chotel Czerwony-Zagórze (Fig. 13). The main objects observed include: the giant intergrowths with massive and palisade structure, top surface of the intergrowths with morphology of crystal apices preserved under the clay cover, synsedimentary dissolution surfaces, selenite regolith and dome composed of giant intergrowths, grass-like facies. (Selenite dome: 50°22′24″ N, 20°43′47″ E)

The 200 m long western outcrop in its southernmost part presents giant gypsum intergrowths with massive and palisade structures, typical of shallow oxygenated brine, with dissolution surfaces, covered with the grass-like gypsum with thin alabaster beds (white fine-crystalline gypsum without clay components), (Fig. 14D). Small isolated intergrowths occur within the grass-like facies. In the north part of this outcrop surface of the giant intergrowths is covered with clay and selenite debris (Fig. 14C); the grass-like gypsum occurs above. Morphology of the crystal apices of the giant intergrowths is excellently preserved in many places under the clay cover. Aggregates of lenticular gypsum crystals resembling the gypsum "roses of desert" occur in clay in pocket-like depressions in the top surface of the giant-crystalline layer, among the selenite crystal clasts and blocks. The same type of contact is seen in the smaller eastern outcrop where a spectacular domal structure composed of giant gypsum intergrowths is seen elevated ca. 90 cm over the average level of the top surface of the giant-crystalline layer (Fig. 14A).

The transition from giant intergrowths to grass-like gypsum represents a shallowing-upwards sequence and emersion. Selenite debris was formed by weathering of the selenite substrate during emersion, when the aggregates of lenticular crystals could grow in clay soaked with Ca-sulphate saturated water. Clay was

deposited from sheet floods of run-off meteoric waters and was carried from emerged land. Clay deposition was controlled by topography of the evaporite shoal. Sheet floods transported mud predominantly along broad depressions of the shoal and covered them with clay. However, on elevated areas (southern part of the western outcrop) fine-crystalline gypsum deposition took place, and the highest of the large gypsum crystals could grow syntaxially because they were free of the clay cover. Just in this way, by syntaxial growth, the selenite dome was formed (Fig. 14B). See more in: Bąbel (1987, 1991b, 1996, 1999a).

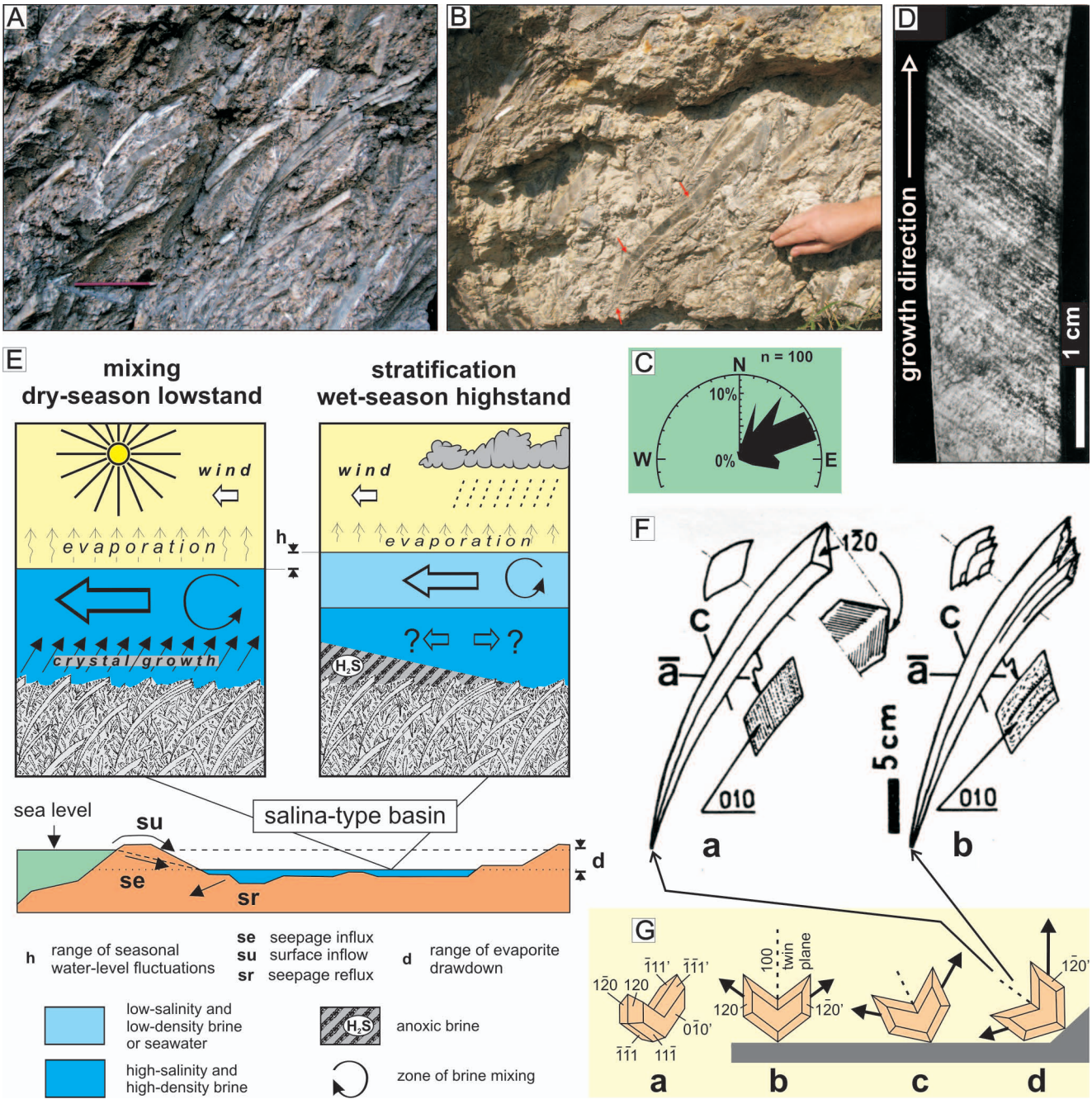

Fig. 11. Sabre facies in abandoned quarry at Siesławice. **A**) Sabre gypsum with conformably oriented crystals, layer *g*. **B**) Conformably oriented sabre crystals with compactional breaks (arrowed, photo by Stefano Lugli), layer *g*. **C**) Rose diagram showing orientation of apices of sabre crystals, layers *g* and *i*, Siesławice (see Fig. 12A), n – number of measurements. **D**) Growth zoning formed by advance of the apical *120* prism in the sabre crystal seen on the *010* cleavage surface in transmitted light. **E**) Interpreted depositional environment and structure of brine column during the growth of oriented sabre crystals (after Bąbel and Becker, 2006, modified). **F**) Sabre crystals growing by advance of the prism faces *120* (a) and lens-shaped subcrystals (b), note different growth structures visible on the *010* cleavage surface. **G**) *100* gypsum twin as a nucleus of the sabre crystals (a), b–d – twinned nuclei growing on the substrate with low chance (b), higher chance (c) and the highest chance (d) to survive the competitive growth.

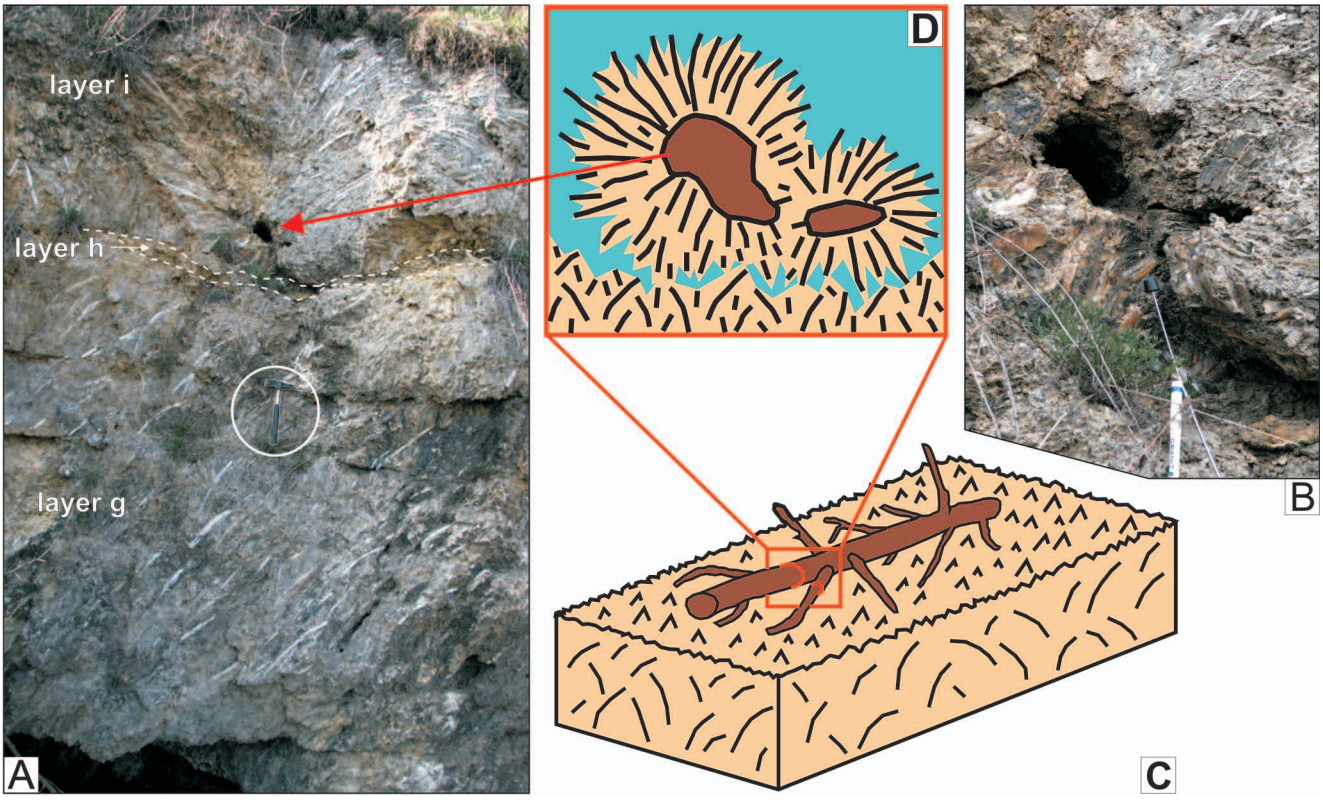

Fig. 12. Tree trunk trace in sabre gypsum, abandoned quarry at Siesławice. **A)** Mould of tree trunk overgrown by gypsum crystals. Sabre crystals show conformable orientation, layers are lettered after Wala (1980). **B)** Mould of tree trunk (and of its side branch?). Detail of A. **C)** Mode of deposition of the drifting tree on basin bottom. **D)** Way of incrustation of the tree by the growing gypsum crystals.

A2.6 Wiślica-Grodzisko, selenite dome composed of sabre gypsum

(50°20′40″ N, 20°40′43″ E)

Leader: Maciej Bąbel

A vertical section through a large selenite dome (one of the several known in this area), is exposed in the wall of an Early Mediaeval fortified settlement (Figs 13, 15A). The competitive growth structures of the sabre crystals seen on the slopes of the dome prove that the crystals grew horizontally in free space, i.e. in brine, on nearly vertical substrate (Fig. 15B, C) and that the dome is a primary form crystallized on the basin bottom. See also: Bąbel (1999a, 2007a), Kasprzyk *et al.* (1999).

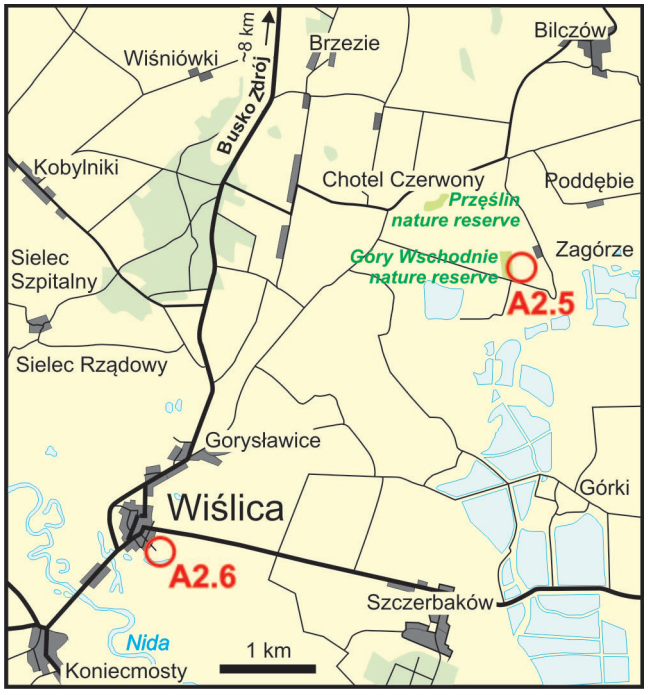

Fig. 13. Detailed location of the field trip stops A2.5 (Chotel Czerwony-Zagórze) and A2.6 (Wiślica-Grodzisko).

A2.7 Borków quarry, complete section of the Nida Gypsum

Leaders: Maciej Bąbel, Krzysztof Nejbert, Danuta Olszewska-Nejbert, Damian Ługowski, Sławomir Gębka[1]

[1]Saint-Gobain Construction Products, Poland (slawomir.gebka@saint-gobain.com)

We visit a working quarry (Fig. 16). Entrance to the quarry requires permission. We observe here: the most complete section of the Nida Gypsum deposits, with nearly all the characteristic Badenian gypsum facies and

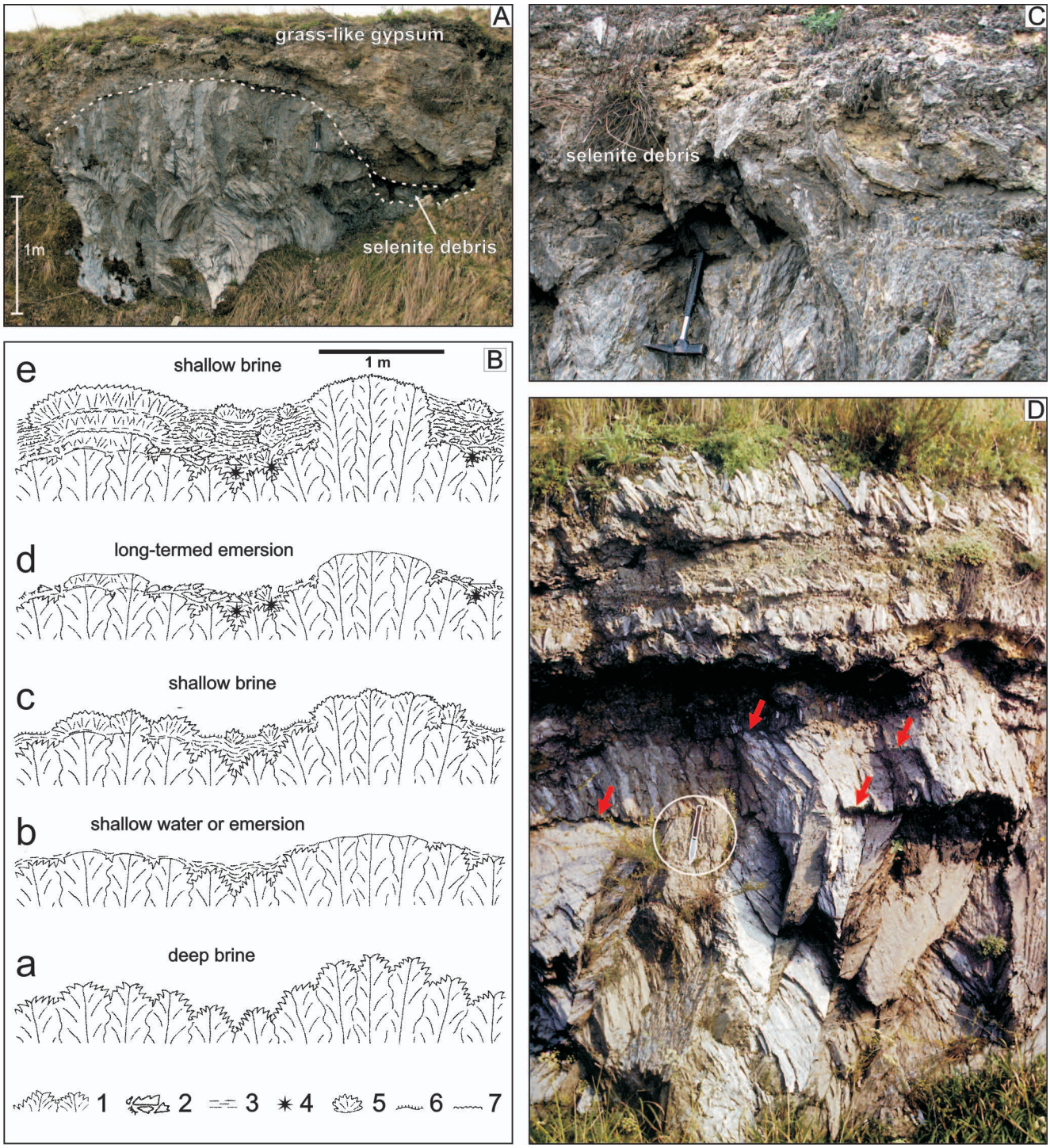

Fig. 14. Outcrops at Chotel Czerwony-Zagórze. **A)** Selenite dome composed of giant intergrowths, and grass-like gypsum, eastern outcrop. **B)** Deposition of selenite debris facies and grass-like gypsum subfacies with clay intercalations during shallowing and emersion of giant gypsum intergrowths (after Bąbel, 1999a): a – palisade growth of giant intergrowths in a deep brine, b – shallowing and influx of meteoric waters with clay; dissolution of highest crystal apices and clay deposition in depressions, c – deposition in shallow brine; growth of grass-like crystals, syntaxial growth of intergrowths, gypsification of microbial mats, d – long-lasting emersion: destruction and weathering of gypsum crystals; growth of lenticular gypsum aggregates in clay-filled depressions, e – deposition in shallow brine; accretion of domal selenitic structures built of grass-like crystals (left) and of giant intergrowths (right), and simultaneous deposition of clay and microbialite gypsum in depressions; 1 – giant gypsum intergrowths; 2 – broken, corroded and abraded gypsum crystals; 3 – clay; 4 – aggregates of lenticular gypsum crystals; 5 – separate aggregates of grass-like gypsum crystals; 6 – wavy-laminated microbial mats encrusted with small gypsum crystals; 7 – gypsified microbial mats with knobby morphology. **C)** Selenite debris covering the giant gypsum intergrowths, western outcrop. **D)** Transition from the massive giant intergrowths subfacies to the grass-like gypsum, synsedimentary dissolution surfaces are arrowed, western outcrop.

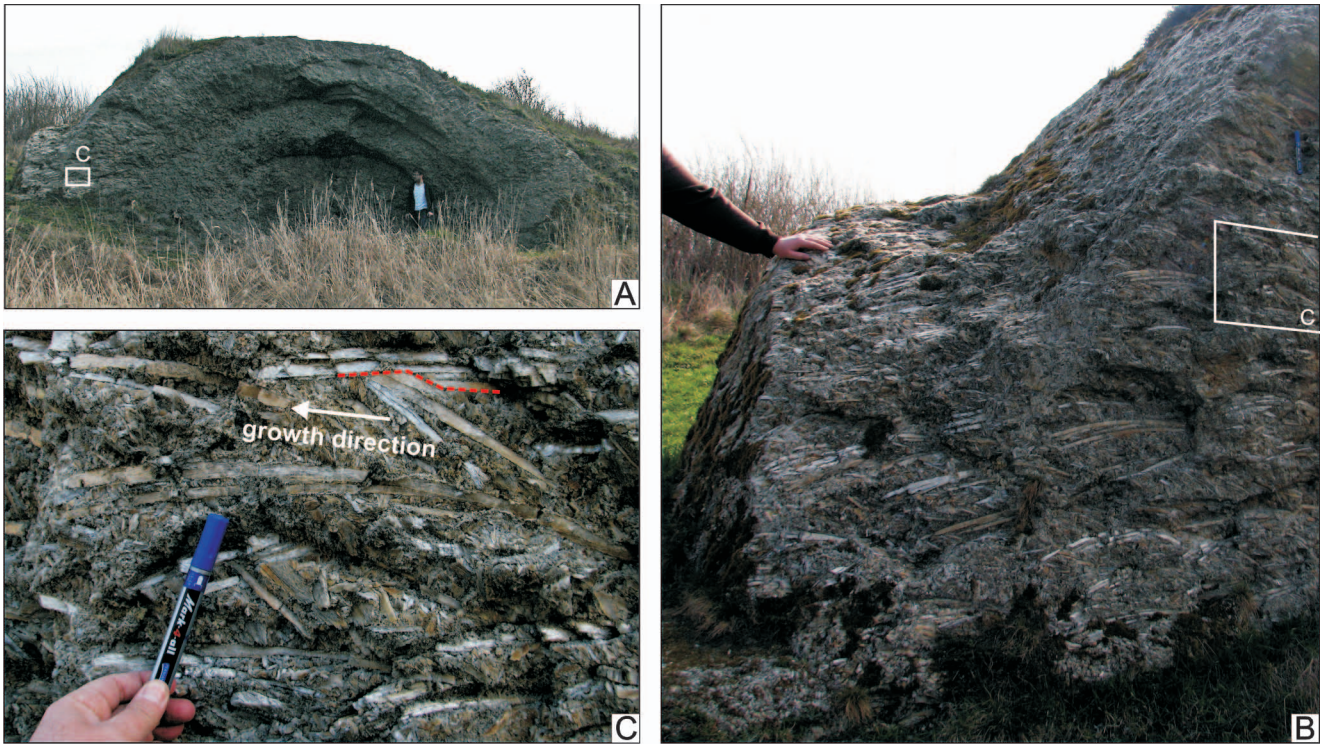

Fig. 15. The giant dome of sabre gypsum, Wiślica-Grodzisko: **A)** general view, **B)** slope of the dome, **C)** detail of A and B, the zig-zag competitive growth (compromise) boundary of the crystals is marked by red dotted line.

sedimentary structures, including selenite and selenite-dominated facies, gypsum microbialites and stromatolites, the clastic, microcrystalline and associated facies with traces of vanished halite. (Entrance to the quarry: 50°33′14″ N, 20°37′40″ E)

This section is the best studied one in the Badenian gypsum basin with respect to geochemistry, sedimentology and palaeontology (Fig. 17; Peryt, 1999; 2013a, b; Peryt and Anczkiewicz, 2015, with references; Peryt and Gedl, 2010; Rosell *et al.*, 1998).

The Badenian marine marls the underlying gypsum in the quarry represent a regional biostratigraphic foraminiferal *Uvigerina costai* zone (D. Peryt, 2013a).

The grass-like subfacies with stromatolitic domes contains flat-topped, up to 32 cm high gypsum domes which were first described from this area as stromatolites by Kwiatkowski as early as in 1970 and 1972 (Fig. 18). They are built of alternating crusts of bottom-grown crystals, gypsified knobby microbial mats and rather smooth laminae of "clastic" sugar-like gypsum. Fenestral pores occur near the bottom-grown crystals. These domes show complex (hybrid), organo-chemical origin. Small grass-like crystals and gypsified microbial mats were formed in a relatively calm environment possibly during salinity oscillations. The sugar-like gypsum was

Fig. 16. Detailed location of the field trip stop at Borków quarry (A2.7).

at least partly deposited mechanically during increased wave and current action. Mechanical deposition is suggested by features of the infilling and flattening of the substrate relief by some of these granular laminae. The grainy laminae run concordantly with dome shapes and also coat the steep slopes of the domes evidently "defying gravity" (Fig. 18C) which suggests that gypsum grains were trapped and bound on such slopes by cohe-

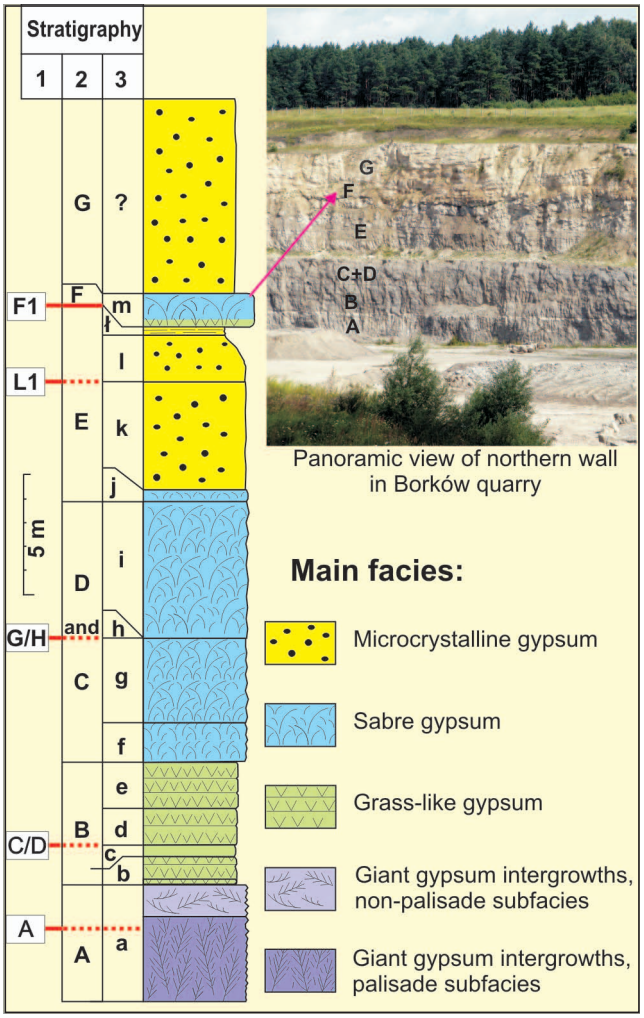

Fig. 17. Simplified geological column of the Badenian gypsum in the Borków quarry. Stratigraphy: 1 – isochronous surfaces after Bąbel (1999b, 2005a), 2 – lithostratigraphic units after Kubica (1992); 3 – layers after Wala (1980).

sive microbial mats (Demicco and Hardie, 1994). Trapping and binding is diagnostic for stromatolites and for microbialites, hence both names: stromatolite and microbialite fit to these laminated parts of the domes. This subfacies could be deposited on a broad windward side of a deeper saline pan, affected by waves and wave currents.

Higher in the section, the sabre facies is present, with crystals predominantly oriented to N and E, and this regionally conformable crystal orientation (see stops A2.1-A2.4 and A2.6) reflects the direction of the brine flow.

The upper clastic unit contains a thin intercalation of grass-like and sabre-like facies with a layer of gypsified microbial mats, a few cm thick, at the base (Figs 5B, 17). Below, there is a clay layer covering the uneven discontinuity surface and containing abundant foraminifers. This clay was interpreted as recording the influx of marine waters and invasion of foraminifers to the evaporite basin (D. Peryt, 2013b). The return to evaporite conditions was recorded by deposition of the selenite-dominated unit above and then the clastic laminated gypsum.

The laminated gypsum deposits covering the described selenite unit contain traces of halite cubes as well as thin layers of halite solution-and-collapse breccias and residual alabaster-like deposits, similar to those from the Leszcze quarry (stop A2.2). The presence of vanished halite proves that water in the basin was episodically saturated with NaCl during clastic gypsum deposition. See also: Bąbel (1991b), Bąbel and Olszewska-Nejbert (2012), Kasprzyk *et al.* (1999), Kowalski (1996), Peryt and Jasionowski (1994), Petryczenko *et al.* (1995).

Acknowledgements. Material presented in this guide is mainly based on the papers by Bąbel (1999a, 2005a) and companion papers (Bąbel, 1999b, 2007b; Bąbel and Becker, 2006; Bąbel and Bogucki, 2007, Bąbel *et al.*, 2010), and partly repeats fragments of the texts and illustrations already published.

References:

Alexandrowicz, S. W., 1967. Pozycja stratygraficzna warstw baranowskich w Woli Zagojskiej koło Pińczowa. *Sprawozdania z Posiedzeń Komisji, Polska Akademia Nauk, Oddział w Krakowie*, 10/1 [for 1966]: 199-202. [In Polish.]

Alexandrowicz, S. W., 1979. Middle Miocene (Badenian) sequence at Górki, southern part of the Korytnica Bay (Holy Cross Mountains, Central Poland). *Acta Geologica Polonica*, 29: 353-361.

Alexandrowicz, S. & Parachoniak, W., 1956. Miocene tuffites in the vicinity of Pińczów on the Nida-river. *Acta Geologica Polonica*, 6: 75-80, 301-325. [In Polish, English summary.]

Anthonissen, E. & Ogg, J. G., 2012. Appendix 3. Cenozoic and Cretaceous biochronology of planktonic foraminifera and calcareous nannofossils. In: Gradstein, F. M., Ogg, J. G., Schmitz, M. D. & Ogg, G. M. (eds), *The Geologic Time Scale 2012*. Elsevier, Amsterdam, pp. 1083-1127.

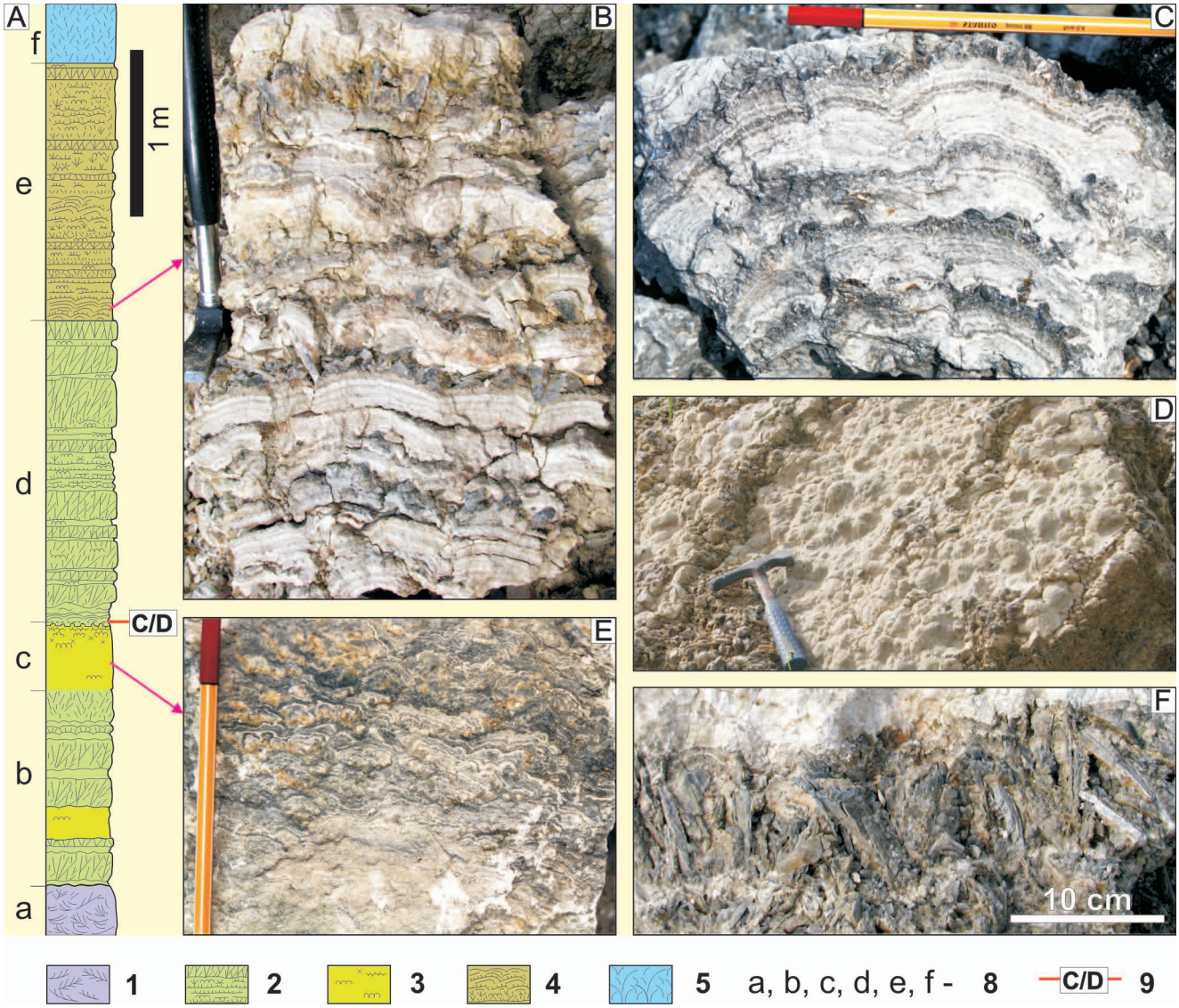

Fig. 18. Grass-like facies and gypsum microbialites in Borków quarry. **A**) Fragment of section containing grass-like facies with gypsum stromatolitic domes, hatchure reflects fabric of gypsum deposits and arrangement of crystals, layers lettered after Wala (1980) – left side, isochronous surface C/D after Bąbel (2005a) – marked on the right. Facies and subfacies: 1 – giant gypsum intergrowths, non-palisade subfacies, 2 – grass-like gypsum, subfacies with crystal rows, 3 – gypsified microbial mats facies, 4 – grass-like gypsum, subfacies with stromatolitic domes, 5 – sabre gypsum facies. **B**) Subfacies with gypsum stromatolitic domes. **C**) Gypsum stromatolitic dome with steep slopes, layer e. **D**) Gypsum microbialite domes over apices of grass-like crystals. **E**) Subfacies with gypsified microbial mats; gypsum cement crystals are honey in colour. **F**) Row of grass-like crystals with large intercrystalline pores.

Bąbel, M., 1986. Growth of crystals and sedimentary structures in the sabre-like gypsum (Miocene, southern Poland). *Przegląd Geologiczny*, 34: 204-208.

Bąbel, M., 1987. Giant gypsum intergrowths from the Middle Miocene evaporites of southern Poland. *Acta Geologica Polonica*, 37: 1-20.

Bąbel, M., 1991a. Crystallography and genesis of the giant intergrowths of gypsum from the Miocene evaporites of Poland. *Archiwum Mineralogiczne*, 44 [for 1990]: 103-135.

Bąbel, M., 1991b. Dissolution of halite within the Middle Miocene (Badenian) laminated gypsum of southern Poland. *Acta Geologica Polonica*, 41: 165-182.

Bąbel, M., 1996. Wykształcenie facjalne, stratygrafia oraz sedymentacja badeńskich gipsów Ponidzia. In: Karnkowski, P. (ed.), *Analiza basenów sedymentacyjnych a nowoczesna sedymentologia, Materiały Konferencyjne V Krajowego Spotkania Sedymentologów*, s. B1-B26. Warszawa. [In Polish.]

Bąbel, M., 1999a. Facies and depositional environments of the Nida Gypsum deposits (Middle Miocene, Carpathian Foredeep, southern Poland). *Geological Quarterly*, 43: 405-428.

Bąbel, M., 1999b. History of sedimentation of the Nida Gypsum deposits (Middle Miocene, Carpathian Fore-

deep, southern Poland). *Geological Quarterly*, 43: 429-447.

Bąbel, M., 2002a. The largest natural crystal in Poland. *Acta Geologica Polonica*, 52: 251-267.

Bąbel, M., 2002b. Brine palaeocurrent analysis based on oriented selenite crystals in the Nida Gypsum deposits (Badenian, southern Poland). *Geological Quarterly*, 46: 435-448.

Bąbel, M., 2004. Badenian evaporite basin of the northern Carpathian Foredeep as a drawdown salina basin. *Acta Geologica Polonica*, 54: 313-337.

Bąbel, M., 2005a. Event stratigraphy of the Badenian selenite evaporites (Middle Miocene) of the northern Carpathian Foredeep. *Acta Geologica Polonica*, 55: 9-29. [On-Line Appendix not attached to the new AGP Home Page is availabe from the author: m.babel@uw.edu.pl]

Bąbel, M., 2005b. Selenite-gypsum microbialite facies and sedimentary evolution of the Badenian evaporite basin of the northern Carpathian Foredeep. *Acta Geologica Polonica*, 55: 187-210.

Bąbel, M., 2007a. Gypsum domes in the karst relief of Ponidzie region, southern Poland. *Prace Instytutu Geografii Akademii Świętokrzyskiej w Kielcach*, 16: 71-89. [In Polish, English summary.]

Bąbel, M., 2007b. Depositional environments of a salina-type evaporite basin recorded in the Badenian gypsum facies in the northern Carpathian Foredeep. In: Schreiber, B. C., Lugli, S. & Bąbel, M. (eds), *Evaporites Through Space and Time. Geological Society, London, Special Publications*, 285: 107-142.

Bąbel, M. & Becker, A., 2006. Cyclonic brine-flow pattern recorded by oriented gypsum crystals in the Badenian evaporite basin of the northern Carpathian Foredeep. *Journal of Sedimentary Research*, 76: 996-1011.

Bąbel, M. & Bogucki, A., 2007. The Badenian evaporite basin of the northern Carpathian Foredeep as a model of a meromictic selenite basin. In: Schreiber, B. C., Lugli, S. & Bąbel, M. (eds), *Evaporites Through Space and Time. Geological Society, London, Special Publications*, 285: 219-246.

Bąbel, M. & Olszewska-Nejbert, D., 2012. Gipsy Borkowa – badeńska sedymentacja ewaporatowa na Ponidziu. In: Skompski, S. (ed.), *Góry Świętokrzyskie. 25 Najważniejszych Odsłonięć Geologicznych*, Wydział Geologii UW, Warszawa, pp. 138-144. [In Polish.]

Bąbel, M., Olszewska-Nejbert, D. & Bogucki, A., 2011. Gypsum microbialite domes shaped by brine currents from the Badenian evaporites of Western Ukraine. In: Reitner, J., Quéric, N.-V. & Arp, G. (eds), *Advances in Stromatolite Geobiology. Lecture Notes in Earth Sciences*, 131: 297-320. Springer, Berlin.

Bąbel, M., Olszewska-Nejbert, D. & Nejbert, K., 2010. The largest giant gypsum intergrowths from the Badenian (Middle Miocene) evaporites of the Carpathian Foredeep. *Geological Quarterly*, 54: 477-486.

Bąbel, M., Urban, J., Chwalik-Borowiec, A. & Łajczak, A., 2013. Stanowisko 6. Gacki: nieczynny kamieniołom gipsów – profil i tektonika serii ewaporatowej, zjawiska krasowe. In: Łajczak, A., Fijałkowska-Mader, A., Urban, J. & Zieliński, A. (eds), *Georóżnorodność Ponidzia*, Wyd. Instytut Geografii UJK w Kielcach, pp. 57-65. [In Polish.]

Becker, A., 2005. Facies development of the Badenian (Middle Miocene) gypsum deposits in the Racławice area (Miechów Upland, southern Poland). *Annales Societatis Geologorum Poloniae,* 75: 111–120.

Bukowski, K., 2011. Badenian saline sedimentation between Rybnik and Dębica based on geochemical, isotopic and radiometric research. *Rozprawy, Monografie*, 236: 1-184. Wyd. AGH, Kraków. [In Polish, English summary.]

Czarnocki, J., 1939. Poszukiwania ropy naftowej w okolicach Wójczy i na obszarach sąsiednich po obu stronach Wisły w r. 1929-31. *Biuletyn Państwowego Instytutu Geologicznego*, 18, Załącznik 1: 1-8. [In Polish.]

Czyżewska, T. & Radwański, A., 1991. Middle Miocene (Badenian) delphinid and phocoenid remains from the Fore-Carpathian Depression in southern Poland. *Acta Geologica Polonica*, 41: 183-191.

de Leeuw, A., Bukowski, K., Krijgsman, W. & Kuiper, K. F., 2010. Age of the Badenian salinity crisis; impact of Miocene climate variability on the circum-Mediterranean region. Geology, 38: 715–718.

Demicco, R. V. & Hardie, L. A., 1994. *Sedimentary Structures and Early Diagenetic Features of Shallow Marine Carbonate Deposits*. SEPM Atlas Series, No. 1: 265 pp. Tulsa, Oklahoma.

Dudek, K. & Bukowski, K., 2004. Badenian pyroclastic levels from Gacki in Nida Valley, Carpathian Foredeep, Poland. *Polskie Towarzystwo Mineralogiczne, Prace Specjalne,* 24: 141-144.

Dudziak, J. & Łuczkowska, E., 1992. Biostratigraphic correlation of foraminiferal and calcareous nannoplankton zones, Early-Middle Badenian (Miocene), Southern

Poland. *Bulletin of the Polish Academy of Sciences, Earth Sciences*, 39 [for 1991]: 199-214.

Garecka, M. & Olszewska, B., 2011. Correlation of the Middle Miocene deposits in SE Poland and western Ukraine based on foraminifera and calcareous nannoplankton. *Annales Societatis Geologorum Poloniae*, 81: 309–330.

Hilgen, F. J., Lourens, L. J., Van Dam, J. A., Beu, A. G., Boyes, A. F., Cooper, R. A., Krijgsman, W., Ogg, J. G., Piller, W. E. & Wilson, D. S., 2012. The Neogene Period. In: Gradstein, F. M., Ogg, J. G., Schmitz, M. & Ogg, G., *The Geologic Time Scale 2012*, Elsevier, Amsterdam, pp. 923-978.

Hohenegger J., Ćorić, S. & Wagreich, M., 2014. Timing of the Middle Miocene Badenian Stage of the Central Paratethys. *Geologica Carpathica*, 65: 55-66.

Jarosiński, M., Poprawa, P. & Ziegler, P. A., 2009. Cenozoic dynamic evolution of the Polish Platform. *Geological Quarterly*, 53: 3-26.

Kasprzyk, A., 1993a. Lithofacies and sedimentation of the Badenian (Middle Miocene) gypsum in the northern part of the Carpathian Foredeep, southern Poland. *Annales Societatis Geologorum Poloniae*, 63: 33-84.

Kasprzyk, A., 1993b. Gypsum facies in the Badenian (middle Miocene) of southern Poland. *Canadian Journal of Earth Sciences*, 30: 1799-1814.

Kasprzyk, A., 1993c. Stromatolitic facies in the Badenian (middle Miocene) gypsum deposits of southern Poland. *Neues Jahrbuch für Geologie und Paläontologie, Abhandlungen*, 187: 375-395.

Kasprzyk, A., 1994. Distribution of strontium in the Badenian (Middle Miocene) gypsum deposits of the Nida area, southern Poland. *Geological Quarterly,* 38: 497-512.

Kasprzyk, A., 1999. Sedimentary evolution of Badenian (Middle Miocene) gypsum deposits in the northern Carpathian Foredeep. *Geological Quarterly*, 43: 449-465.

Kasprzyk, A. & Ortí, F., 1998. Palaeogeographic and burial controls on anhydrite genesis: the Badenian basin in the Carpathian Foredeep (southern Poland, western Ukraine). *Sedimentology*, 45: 889-907.

Kasprzyk, A., Peryt, T. M., Turchinov, I. I. & Jasionowski, M., 1999. Badenian gypsum in the Ponidzie area, the northern Carpathian Foredeep, Poland. *International Conference "Carpathian Foredeep Basin – its evolution and mineral resources"*, Excursion 5, Kraków, 21 pp.

Khrushchov, D. P. & Petrichenko, O. I., 1979. Evaporite formations of Central Paratethys and conditions of their sedimentation. *Annales Géologiques des Pays Helléniques*, Tome hors série, No. 2: 595-612.

Kováč, M., Andreyeva-Grigorovich, A.S., Bajraktarević, Z., Brzobohatý, R., Filipescu, S., Fodor, L., Harzhauser, M., Nagymarosy, A., Oszczypko, N., Pavelić, D., Rögl, F., Saftić, B., Sliva, L. & Studencka, B., 2007. Badenian evolution of the Central Paratethys Sea: paleogeography, climate and eustatic sea-level changes. *Geologica Carpathica*, 58: 579–606.

Kowalski B. J. 1996. Young tectonic faulting in the Borków area, Nida Basin near Pińczów. *Prace Instytutu Geografii WSP w Kielcach*, 1: 129-146. [In Polish, English summary.]

Krysiak, Z., 2000. Tectonic evolution of the Carpathian Foredeep and its influence on Miocene sedimentation. *Geological Quarterly,* 44: 137-156.

Kubica, B., 1992. Lithofacial development of the Badenian chemical sediments in the northern part of the Carpathian Foredeep. *Prace Państwowego Instytutu Geologicznego*, 133: 1-64. [In Polish, English summary.]

Kwiatkowski, S., 1970. Origin of alabasters, intraformational breccias, folds and stromatolites in Miocene gypsum of Southern Poland. *Bulletin de l'Académie Polonaise des Sciences, Sér. Sciences Géologiques et Géographiques*, 18: 37-42.

Kwiatkowski, S., 1972. Sedimentation of gypsum in the Miocene of southern Poland. *Prace Muzeum Ziemi*, 19: 3-94. [In Polish, English summary.]

Łuczkowska, E., 1974. The Miocene profile in the exposure at Gacki near Pińczów. *Sprawozdania z Posiedzeń Komisji Naukowych, PAN, Oddział w Krakowie*, 17/1 [for 1973]: 192-194. [In Polish.]

Lugli, S., Manzi, V., Roveri, M. & Schreiber, B. C., 2010. The Primary Lower Gypsum in the Mediterranean: A new facies interpretation for the first stage of the Messinian salinity crisis. *Palaeogeography, Palaeoclimatology, Palaeoecology*, 297: 83–99.

Łyczewska, J., 1972. *Objaśnienia do Szczegółowej Mapy Geologicznej Polski, Arkusz Busko Zdrój, 1:50 000*. Wydawnictwa Geologiczne, Warszawa, 58 pp. [In Polish.]

Mutti, E. & Ricci Lucchi, F., 1975. Turbidite facies and facies associations. In: E. Mutti, E., Parea, G. C., Ricci Lucchi, F., Sagri, M., Zanzucchi, G., Ghibaudo, G. & Jaccarino, S. (eds), *Field trip guidebook A-11, Examples of turbidite facies and facies associations from selected formations of*

the Northern Apennines, 9th IAS Congress, Nice, France, pp. 21-36.

Niemczyk, J., 2005. Outline of the gravitational tectonic in the Miocene gypsum formation of the Carpathian foreland in Poland. *Geologia, Kwartalnik AGH*, 31: 75–126. [In Polish, English summary.]

Osmólski, T., 1972. The influence of the geological structure of the marginal parts of the Działoszyce trough on the metasomatosis of gypsum. *Biuletyn Instytutu Geologicznego*, 260: 65-188. [In Polish, English summary.]

Osmólski, T., Krysiak, Z. & Wilczyński, M. S., 1978. New data on the Kurdwanów - Zawichost zone and the tectonics of the area between Busko and Nida and Vistula. *Kwartalnik Geologiczny*, 22: 833–850. [In Polish, English summary.]

Oszczypko, N., Krzywiec, P., Popadyuk, I. & Peryt, T., 2006. Carpathian Foredeep Basin (Poland and Ukraine): its sedimentary, structural, and geodynamic evolution. In: Golonka, J. & Picha, F. J. (eds), *The Carpathians and their foreland: Geology and hydrocarbon resources. AAPG Memoir*, 84: 293-350.

Oszczypko, N. & Tomaś, A., 1977. Fossil zones of weathering in Cretaceous and Jurassic sediments of the central part of Carpathian Foreland. *Sprawozdania z Posiedzeń Komisji Naukowych, Polska Akademia Nauk, Oddział w Krakowie*, 20/1 [for 1976]: 1940-1941. [In Polish.]

Paruch-Kulczycka, J., 2015. Foraminiferal biostratigraphy of the Miocene deposits from the Busko (Młyny) PIG-1 and Kazimierza Wielka (Donosy) PIG-1 boreholes (northern part of the Carpathian Foredeep). In: Czapowski, G. & Gąsiewicz, A. (eds), Paleogene and Neogene of Poland – new data. *Biuletyn Państwowego Instytutu Geologicznego*, 461: 115-131. [In Polish, English summary.]

Peryt, D., 1999. Calcareous nannoplankton assemblages of the Badenian evaporites in the Carpathian Foredeep. *Biuletyn Państwowego Instytutu Geologicznego*, 387: 158-161.

Peryt, D., 2013a. Foraminiferal record of the Middle Miocene climate transition prior to the Badenian salinity crisis in the Polish Carpathian Foredeep Basin (Central Paratethys). *Geological Quarterly*, 57: 141-164.

Peryt, D., 2013b. Foraminiferal record of marine transgression during deposition of the Middle Miocene Badenian evaporites in Central Paratethys (Borków section, Polish Carpathian Foredeep). *Terra Nova*, 25: 298-306.

Peryt, D. & Gedl, P., 2010. Palaeoenvironmental changes preceding the Middle Miocene Badenian salinity crisis in the northern Polish Carpathian Foredeep Basin (Borków quarry) inferred from foraminifers and dinoflagellate cysts. *Geological Quarterly*, 54: 487-508.

Peryt, T. M., 1996. Sedimentology of Badenian (middle Miocene) gypsum in eastern Galicia, Podolia and Bukovina (West Ukraine). *Sedimentology*, 43: 571-588.

Peryt, T. M., 2001. Gypsum facies transitions in basin-marginal evaporites: middle Miocene (Badenian) of west Ukraine. *Sedimentology*, 48: 1103-1119.

Peryt, T. M., 2006. The beginning, development and termination of the Middle Miocene Badenian salinity crisis in Central Paratethys. *Sedimentary Geology*, 188–189: 379–396.

Peryt, T. M., 2013. Palaeogeographical zonation of gypsum facies: Middle Miocene Badenian of Central Paratethys (Carpathian Foredeep in Europe). *Journal of Palaeogeography*, 2: 225-237.

Peryt, T. M. & Anczkiewicz, R., 2015. Strontium isotope composition of Middle Miocene primary gypsum (Badenian of the Polish Carpathian Foredeep Basin): evidence for continual non-marine inflow of radiogenic strontium into evaporite basin. *Terra Nova*, 27: 54–61.

Peryt, T. M. & Jasionowski, M., 1994. In situ formed and redeposited gypsum breccias in the Middle Miocene Badenian of southern Poland. *Sedimentary Geology*, 94: 153-163.

Peryt, T. M. & Kasprzyk, A., 1992. Earthquake-induced resedimentation in the Badenian (middle Miocene) gypsum of southern Poland. *Sedimentology*, 39: 235-249.

Petrichenko, O. I., Peryt, T. M. & Poberegsky, A. A., 1997. Pecularities of gypsum sedimentation in the Middle Miocene Badenian evaporite basin of Carpathian Foredeep. *Slovak Geological Magazine*, 3: 91-104.

Petryczenko, O. I., Peryt, T. M., Pobereżski, A. W. & Kasprzyk, A., 1995. Inclusions of microorganisms in the Middle Miocene Badenian gypsum crystals of the Carpathian Foredeep. *Przegląd Geologiczny*, 43: 859-862. [In Polish, English summary.]

Połtowicz, S., 1993. Palinspastic palaeogeography reconstrution of Badenian saline sedimentary basin in Poland. *Geologia, Kwartalnik*, 19: 174–178, 203–233. [In Polish, English summary.]

Remin, Z., 2004. Biostratigraphy of the Santonian in the

SW margin of the Holy Cross Mountains near Lipnik, a potential reference section for extra-Carpathian Poland. *Acta Geologica Polonica*, 54: 587-596.

Rouchy, J. M. & Caruso, A., 2006. The Messinian saliniy crisis in the Mediterranean basin: a reassessment of the data and an integrated scenario. *Sedimentary Geology*, 188–189: 35–67.

Rosell, L., Ortí, F., Kasprzyk, A., Playa, E. & Peryt, T. M., 1998. Strontium geochemistry of Miocene primary gypsum: Messinian of southeastern Spain and Badenian of Poland. *Journal of Sedimentary Research*, 68: 63-79.

Rögl, F., 1999. Mediterranean and Paratethys. Facts and hypotheses of an Oligocene to Miocene paleogeography (short overview). *Geologica Carpathica*, 50: 339-349.

Rutkowski, J., 1981. The tectonics of the Miocene sediments of the western part of Połaniec Graben (Carpathian Foredeep. Southern Poland). *Annales Societatis Geologorum Poloniae*, 51: 117-131. [In Polish, English summary.]

Ślączka, A. & Kolasa, K., 1997. Resedimented salt in the Northern Carpathians Foredeep (Wieliczka, Poland). *Slovak Geological Magazine*, 3: 135-155.

Śliwiński, M., Bąbel, M., Nejbert, K., Olszewska-Nejbert, D., Gąsiewicz, A., Schreiber, B. C., Benowitz, J. A. & Layer, P., 2012. Badenian–Sarmatian chronostratigraphy in the Polish Carpathian Foredeep. *Palaeogeography, Palaeoclimatology, Palaeoecology*, 326-328: 12–29.

Urbaniak, J., 1985. New data for stratigraphy of Miocene alabaster gypsum deposit at Łopuszka Wielka near Kańczuga. *Przegląd Geologiczny*, 23: 121-126. [In Polish, English summary.]

Wala, A., 1980. Litostratygrafia gipsów nidziańskich (fm). In: *Symp. naukowe „Gipsy niecki nidziańskiej i ich znaczenie surowcowe"*. Printed manuscript, Kraków, 6pp.

Wagreich, M., Hohenegger, J. & Ćorić, S., 2014. Base and new definition of the Lower Badenian and the age of the Badenian stratotype (Middle Miocene, Central Paratethys). In: Rocha, R., Pais, J., Kullberg, J. C. & Finney, S. (eds), STRATI 2013, *First International Congress on Stratigraphy, At the Cutting Edge of Stratigraphy*, Springer, Cham, pp. 615-618.

Warren, J. K., 2006. *Evaporites: Sediments, Resources and Hydrocarbons. Springer*, Berlin, 1035 pp.

Appendix.

Facies of the Nida Gypsum deposits and their sedimentary environments; after Bąbel (1999a, 2005b), supplemented. The Badenian gypsum facies were also described and reviewed by Kasprzyk (1993a, b; 1999), Kubica (1992), T. Peryt (1996, 2001, 2013), Petrichenko *et al.* (1997).

Facies	Main depositional mechanism	Subfacies	Stops; illustrations	Inferred depositional environment	Selected references
Carbonate facies	Diagenetic processes	—		—	—
Porphyroblastic gypsum	Diagenetic processes	—		—	—
Microcrystalline gypsum	Mechanical deposition Gravity flows, halite-solution collapse, Residual gypsum accumulation after halite solution, cohesive flows and slumps Periodic settling of redeposed and precipitating gypsum crystals from brine column, clay and gypsum mud suspension fallout	Breccias Alabasters Laminated gypsum	A2.2, A2.7; Figs 8E, F	Brackish-to-saline perennial pan with fluctuating salinity	Kwiatkowski, 1972, Peryt & Kasprzyk, 1992
Selenite debris flow	Debris flow		A2.3; Fig. 9C	Slope of the saline gypsum pan	Bąbel, 2005b
Sabre gypsum	Syntaxial bottom growth of crystals with common creation of new crystals	Wavy bedded Flat bedded	A2.1, A2.2, A2.3, A2.4, A2.6, A2.7; Figs 14A, C; 18A, B	Density stratified monomictic saline pan with Ca-sulphate saturated brine of high salinity	Bąbel, 1986, Kasprzyk, 1993 a, b; Petryczenko et al., 1995; Bąbel & Becker, 2006, Bąbel & Bogucki, 2007
Grass-like gypsum	Alternated syntaxial bottom growth of crystals and deposition of fine-crystalline gypsum	Subfacies with stromatolitic domes Subfacies with crystal rows Subfacies with alabaster beds Subfacies with clay intercalations	A2.2, A2.3, A2.5, A2.7; Figs 14A, D; 18B, C, F	Semi-emerged evaporitic shoals passing into shallow saline pans (with Ca-sulphate saturated brine) and coastal clay-gypsum flats	Bąbel, 1999a
Gypsum microbialites	Microbialite deposition	Gypsified microbial mats	A2.2, A2.3, A2.7; Figs 14B, C	Semi-emerged evaporite shoal covered with microbial mats	Kwiatkowski, 1970, 1972; Kasprzyk, 1993c; Bąbel, 1999a, 2007; Bąbel et al., 2010
Selenite debris	Weathering		A2.2, A2.3, A2.5; Fig. 14C	Semi-emerged clay-gypsum (sabkha-like) flat	Bąbel, 1999a, 2005b
Giant intergrowths	Syntaxial bottom growth of crystals with rare creation of new crystals	Non-palisade intergrowths Palisade intergrowths (skeletal and massive) Clay subfacies	A2.1, A2.2, A2.3, A2.5, A2.7; Figs 7A, B; 8B; 9B; 14A, C, D	Density stratified saline pan with Ca-sulphate saturated brine of low salinity	Bąbel, 1987, 1991a; Peryt, 1996

The Organizing Committee would like to acknowledge the generous support of our Sponsors, Patrons, Partners and Exhibitors

Ministry of Science and Higher Education
Republic of Poland

Platinum Sponsor

ORLEN Upstream

Silver Partner

PGNiG
Polish Oil & Gas Company

Silver Sponsor

Springer

Patron

WIELICZKA SALT MINE

USB Flash-Drive Sponsor

WILEY

Writing-Pad & Writing-Pen Sponsor

SHALETECH ENERGY

Patron Sponsor

BETA
Radiocarbon Dating
Consistent Accuracy Delivered On-Time
Beta Analytic Ltd.

CoCaRDE

European Science Foundation

ZGM Bolesław

Muszynianka
naturalna woda mineralna

Lanyard Sponsor

ZEISS

Exhibitors

geokrak

SYL & ANT Instruments

INTROLIGATORNIA
Wiesław Nowotarski


2015
KRAKÓW